AN ANALYTIC MODEL FOR THE ELECTROSTATIC CONTRIBUTION OF THE ELECTRON CLOUD TO THE VERTICAL TUNE-SHIFT

Levi Schächter*, Cornell University, Ithaca, NY 14853, USA

Abstract

An analytic quasi-static model is developed for the analysis of the tune-shift associated with the presence of an electron cloud in a damping ring. Its essence is to assume that, from the perspective of a given bunch, it experiences, in average over one turn, a uniform cloud in the direction of motion. However, each bunch experiences a different cloud density. Another essential component of the model is the cloud's life-time. It controls the build-up, the equilibrium and the decay of the cloud. In case of a train of positron bunches, electrons may be trapped in the vertical direction for the entire train duration. Tacitly it is assumed that the ring is dominated by vertical magnetic fields due to either bends or wigglers.*

INTRODUCTION

As multi-GeV bunches of electrons or positrons circulate in damping rings, they generate synchrotron radiation which is essential for the particles' cooling process. When hitting the metallic walls, this radiation generates photo-electrons. An additional process, that may generate a substantial amount of free electrons in the beam-chamber, is the ionization of the residual gas (primarily hydrogen). A third mechanism responsible to the presence of free-electrons in the beam-chamber is secondary emission occurring when electrons impinge upon the metallic wall. Finally, stray particles from the bunch may also generate free-electrons. Referred to as "electron-cloud" (EC) all these free-electrons, energized directly by the bunches or by the wake-field, may have a detrimental effect on the operation of a damping ring. In fact, since in zero order all the processes mentioned above are proportional to the number of particles in each bunch, the problem becomes more and more severe as the number of particles is increased.

And indeed, the EC effect on positrons was first detected in 1995 [1], at KEK when attempting to increase significantly the average current of a train of positron bunches. A first explanation of the process was presented by Ohmi [2] a couple of months after the publication of the experimental result, attributing the vertical coupled-bunch instability to the photo-electrons. While the cloud generation is a result of the multi-bunch process, the impact of the cloud back on the positrons can be on the entire train but it may also affect dramatically the single-bunch shape via the head-tail instability [3]. An excellent summary of the experimental results accumulated throughout the years has been put together by Fukuma [4] to which we should add the recent observation of vertical betatron sideband again, attributed to the EC [5]. A large variety of simulation codes have been developed and/or employed for the analysis of the various phenomena associated with the electron cloud. A review of the various possibilities is beyond the scope of this study however, it warrants to point out that a summary of a comparative study has been published recently by Hofmann [6] and yet new results from plasma oriented codes, enlighten new aspects of the electron-cloud effects [7].

In the framework of this study we describe an analytic model which in conjunction with experimental data (vertical tune-shift) provides a self-consistent picture of the build-up, trapping and decaying of electrons in a ring which is dominated by bends and wigglers namely, vertical magnetic field as is the case in Cornell Electron/positron Storage Ring (CESR).

BASIC MODEL

The electron-cloud phenomenon is a delicate balance between generation of electrons and the natural absorption of charge at the metallic wall. This balance is complicated by the magnetic field associated with the lattice, by energy delivered by bunches and by the overall space-charge effect. In spite the difficulties accompanied by an exact account of each one of these effects, we postulate the existence of a cloud in a fraction of the beam-chamber adjacent to the outer vertical wall. For simplicity sake, the beam-chamber is assumed to be rectangular $\left(D_x \times D_y\right)$ and vertical symmetry of the cloud will be assumed throughout the discussion – see Figure 1.

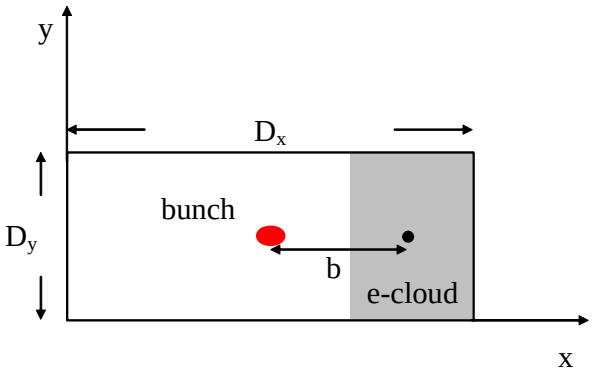

Figure 1: Schematics of a rectangular beam-chamber with the electron (or positron) bunch in the center and the electron cloud filling part of the volume of the chamber.

* On Sabbatical from the Technion – Israel Institute of Technology
email: levi@ee.technion.ac.il
Research supported by the DoE and NSF

The cloud is assumed to fill the vertical dimension uniformly whereas in the horizontal direction it only partially fills the space – its size is conveniently described in terms of the distance (b) between its center-of-mass and the center of the beam-chamber; for $b = 0$ the cloud uniformly fills the entire chamber whereas at the limit $b \to D_x/2$ it occupies an infinitely small region close to the vertical wall which is the direct target of the synchrotron radiation. In practice, what is sufficient for this model to work, is to assume that the cloud is symmetric relative to the horizontal axis. A distribution different than the uniform one prescribed above will only introduce one more degree of freedom in the model but the essence will remain unchanged. Before proceeding it is important to make two comments: (i) each segment of a damping ring is different and so is the contribution of each one of the processes mentioned in the Introduction. (ii) As it will be discussed subsequently, in the present model we consider the effective cloud configuration *as experienced by each bunch* separately.

Along the circumference (C) of the ring a train of N_b bunches of spacing T, each bunch consisting of N_e electrons (or positrons), generates in the beam chamber a cloud of an *average density* n_{ec} -- thus the total charge in the cloud may be assumed to be $Q_0 = en_{ec}CD_xD_y$.

BUILD-UP

In case of a train of bunches it is essential to establish the electron-cloud density experienced by each bunch in the train. For this purpose, it is necessary to envision the EC as a dynamic equilibrium of two processes: on the one hand electrons are absorbed at the wall at a rate which is proportional to the density and inversely proportional to some characteristic life-time τ which is yet to be determined -- a realistic estimate of this life-time is one of the main goals of this study. On the other hand, during each bunch passage, a certain number of "new-born" electrons are generated. Consequently, denoting by $n_\nu^{(nb)}$ the average density of the new-born electrons attributed to bunch ν, the cloud density due to a train of N_b bunches is determined by

$$\frac{dn_{ec}}{dt} + \frac{n_{ec}}{\tau} = \sum_{\nu=1}^{N_b} n_\nu^{(nb)} \delta\left(t - \nu T\right) \qquad (1)$$

here it is tacitly assumed that the bunch length is much shorter than the bunch spacing thus the former may be represented by a point-charge (delta-function). In principle, the new-born electrons include all four mechanisms mentioned above. Figure 2 illustrates both the build-up, the equilibrium and the decaying process of the normalized density $\bar{n} = n_{ec}/n_{nb}$ assuming that all twenty bunches are identical.

Each bunch contributes its portion to the cloud thus the new-born electrons add to earlier generated ones but at the same time, they start to be absorbed at the wall. Equilibrium is reached when the two processes (generation and absorption) balance each other. In fact, assuming that equilibrium is reached, its value is approximately

$$n_{ec}^{(eq)} \simeq n_{nb}\frac{\tau}{T} \qquad (2)$$

and the "envelope" of the build-up, equilibrium and decay of the cloud may be described by

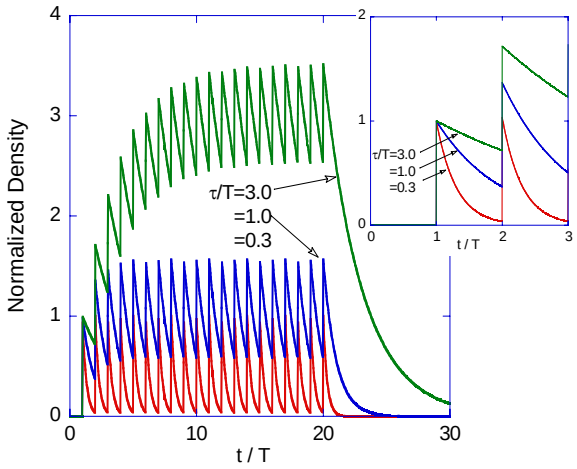

Figure 2: Build-up, equilibrium and decaying process in the cloud.

$$n_{ec}(t) \simeq n_{nb}\frac{\tau}{T}\left[1-\exp\left(-\frac{t}{\tau}\right)\right]\left[h(t)-h(t-NT)\right] + n_{nb}\frac{\tau}{T}\exp\left(-\frac{t-NT}{\tau}\right)h(t-NT) \qquad (3)$$

tacitly assuming that life-time is longer than the bunch spacing ($\tau > T$). If this were not the case, there is no significant build-up of the cloud; $h(t)$ is the Heaviside step-function. It is important to point out that during the first few bunches the build-up is, within a good approximation, linear in time (or in bunch index) and independent of the life-time; its slope being determined by the bunch spacing. As discussed subsequently, this trend has been observed experimentally at CESR.

In zero-order, the density of new-born electrons may be assumed to be *proportional* to the number of electrons in the bunch (and thus to the average current - $I_\nu = eN_{e,\nu}c/C$). As a result $n_\nu^{(nb)} / \left\langle n_\mu^{(nb)} \right\rangle_\mu \simeq I_\nu / \langle I \rangle$ wherein $\langle \ldots \rangle$ denotes averaging over all the bunches in the train.

A solution of (1) subject to the assumption that the life-time is independent of the cloud density is simple and it allows to establish the *density experienced by each bunch* which is what counts from the perspective of the measurement namely,

$$n_{ec,\mu} \equiv n_{ec}\left(t = \mu T - 0\right) = n_{nb}\sum_{\nu=1}^{N}\frac{I_\nu}{\langle I \rangle}h(\mu-\nu-0)\exp\left[-\frac{T}{\tau}(\mu-\nu)\right]; \qquad (4)$$

here $n_{nb} = \left\langle n_{\mu}^{(nb)} \right\rangle$ is the average density of new-born electrons averaged over all the bunches in the train. The zero in the argument of the step-function emphasizes the fact that the bunch experiences only the cloud generated by its *preceding* counterparts but not the electrons itself generates. This expression will subsequently play an important role in the framework of our model.

LIFE-TIME W/O BUNCH KICK

So far the life-time was conceived to be an independent parameter. In practice, the life-time of a "new-born" electron is related to the parameters of the cloud (density and geometry), the beam-chamber geometry and obviously on the train of bunches. Moreover, this parameter is expected to vary significantly from one element of the ring to another according to the typical magnetic field. At one extreme, the wigglers which virtually limit significantly any net horizontal or longitudinal motion of the electrons. And at the other extreme, the straights, where no confining magnetic field is present and "new-born" electrons are free to move.

Confining the motion to the vertical direction implies that these electrons can not originate from *direct* impact of synchrotron radiation on the wall (the latter will hit the vertical rather than the horizontal wall). Photo-electrons or secondary-electrons may however cross the magnetic field lines if a significant *longitudinal* electric field is present resulting into an $E \times B$ drift (the latter being the vertical magnetic field). Such an electric field may be due to either the direct electric field of the bunch or the wake generated by the bunch along the structure.

Along the magnetic field lines if the original energy of a photo-electron is E, then the "ballistic" time (τ_b) it takes it to traverse a vertical gap D_y is given by $\tau_b(E) \equiv (D_y / c)\sqrt{V_e / 2E[eV]}$ with $V_e = 0.511[MeV]$. Thus for $D_y = 5[cm]$ and 400[eV] this ballistic time is $\tau_b \sim 4[n\text{sec}]$ these being electrons relatively close to the peak of secondary emission (300eV). For low energy electrons (1[eV]) the ballistic time is of the order of $\tau_b \sim 80[n\text{sec}]$. While the ballistic-electron approximation hints in what energy range the cloud electrons are, it is by no means a reasonable approximation since a significant fraction of the energy associated with each new-born electron is converted into electrostatic (potential) energy.

For an estimate of the life-time in the presence of the electron cloud, but ignoring (momentarily) the impact of the bunches, the dynamics is governed by the plasma frequency of the cloud hence

$$\left[\frac{d^2}{dt^2} - \Omega_p^2\right]\delta y_i = 0 \qquad (5)$$

with $\delta y_i = y_i - D_y / 2$, $\Omega_p^2 = \left(e^2 n_{ec} / m\varepsilon_0\right) f_P\left(\bar{b}\right)$ and the form-factor, $f_P\left(\bar{b}\right)$, for the specific cloud configuration is calculated in Appendix A. This equation has a simple solution of the form

$$\delta y_i(t) = \delta y_i(0)\cosh\left(\Omega_p t\right) + \Omega_p^{-1}\delta \dot{y}_i(0)\sinh\left(\Omega_p t\right) \qquad (6)$$

and without loss of generality, it is assumed that an electron starts its motion from the *lower* plane $\delta y_i(0) = -D_y / 2$ with an initial velocity $\delta \dot{y}_i(0) = \sqrt{2E_i / m}$ where E_i is the energy the electron is injected into the gap. The time (τ_i) it takes the electron to reach the *upper* plane is determined from the condition $\tanh\left(\Omega_p \tau_i / 2\right) = \sqrt{E_p / E_i}$ with $E_P \equiv (m/2)\left(\Omega_p D_y / 2\right)^2$ denoting the potential energy associated with electron cloud. Evidently, an electron reaches the upper plane only if its kinetic energy is greater than the potential energy $\left(E_i > E_p\right)$. In the opposite case, the electron bounces back and its life time may be calculated by evaluating the time it reaches zero (vertical) velocity – see Appendix A. Combining the two results we conclude that the time an electron of an initial energy E_i, spends in the vacuum-chamber, ignoring the bunch(es) kick, is

$$\tau_i = \tau'(E_i) = \frac{2}{\Omega_p}\begin{cases} \operatorname{atanh}\left(\sqrt{E_i / E_p}\right) & E_i < E_p \\ \operatorname{atanh}\left(\sqrt{E_p / E_i}\right) & E_i > E_p. \end{cases} \qquad (7)$$

For evaluation of the *average* life-time it is assumed that the electron's spectrum is *uniform* between zero and E_0, implying that the average energy is $\langle E \rangle = E_0 / 2$ and therefore the average life-time in terms of the average energy is

$$\tau = \frac{1}{E_0}\int_0^{E_0} dE\,\tau'(E) = \frac{2}{\Omega_p} g\left(2\frac{\langle E \rangle}{E_p}\right) \qquad (8)$$

with $g(x)$ defined in (57) of Appendix A.

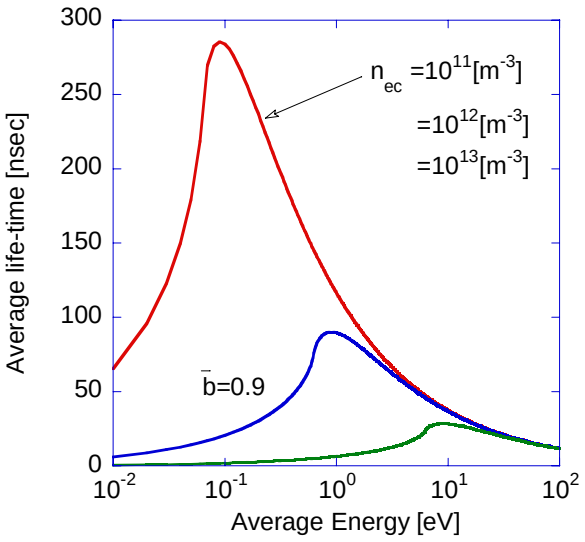

Figure 3: Life-time as a function of the average energy of the cloud for $\bar{b} = 0.9$ and $n_{ec} = 10^{11}, 10^{12}, 10^{13}[m^{-3}]$.

Figure 3 illustrates the variation of the life-time as a function of the average energy of the cloud for three cloud densities: $n_{ec} = 10^{11}, 10^{12}, 10^{13}[m^{-3}]$. At high average energies (ballistic regime) the life-time becomes independent of the cloud density and it approaches zero. It diminishes again at very low energies since the electron is reflected immediately back to the wall. In between, there is a peak which may be significantly longer than the typical ballistic life-time and clearly it can be attributed to these electrons of the spectrum which have an initial energy close to that of the potential energy of the cloud. Obviously this peak is dependent on the cloud density and for $n_{ec} \simeq 10^{11}[m^{-3}]$ this peak life-time is close to 300 nsec however, it drops to less than 25 nsec if the density increases to $n_{ec} \simeq 10^{13}[m^{-3}]$; in all three cases $\bar{b} = 0.9$ which means that the cloud occupies a thin layer close to the outer vertical wall.

LIFE-TIME WITH BUNCH KICK

An additional complication in the dynamics of an electron in the cloud is associated with the presence of the bunches. They generate two electromagnetic fields that may affect the motion of the electrons in the cloud: the self-field attached to the bunch and the wake trailing long after the bunch. In what follows, it is assumed that the former is dominant and in addition, except if otherwise specified, it is assumed that the bunch consists of positrons.

Each positron bunch (ν) affects the electrons in the cloud by delivering a kick which may be shown to be given by

$$\left.\frac{d\delta y_i}{dt}\right|_{t=\nu T+0} - \left.\frac{d\delta y_i}{dt}\right|_{t=\nu T-0} = -\Omega_{K,\nu}\,\delta y_i|_{t=\nu T} \qquad (9)$$

where in Appendix B it is demonstrated that the "kick-frequency", for the specific cloud geometry assumed above, is given by

$$\Omega_{K,\nu}^2 = \left(\frac{e^2 N_{e,\nu}}{m\varepsilon_0 D_y^3}\frac{D_y}{c}\right)^2 \frac{96/\pi^4}{\left(1-\bar{b}\right)^2} \times \sum_{n_y=1}^{\infty}\left\{\sum_{n_x=1}^{\infty}\frac{\sin\left(\frac{\pi}{2}n_x\right)\sin\left(\frac{\pi}{2}n_y\right)}{\frac{n_x}{n_y}\left(n_x^2\frac{D_y}{D_x}+n_y^2\frac{D_x}{D_y}\right)}\Lambda_{n_x}\right\}^2 \qquad (10)$$

where the form-factor is $\Lambda_{n_x} = \cos\left(\pi n_x \bar{b}\right) - \cos\left(\pi n_x\right)$. In case of electrons bunch, the expression in the right hand side term of (9) *reverses* sign. In addition, assuming that globally the cloud is stationary, the average kinetic energy, is

$$\Delta E_{\mathrm{kick},\nu} = \frac{m}{2}\left(\frac{\Omega_{K,\nu} D_y}{2\sqrt{3}}\right)^2 \qquad (11)$$

regardless whether the individual bunch consists of electrons or positrons. For the typical set of parameters at CESR, this energy is depicted in Figure 4 ($N_e = 10^{10}$) and three facts are noticeable: first, even if the cloud fills the entire chamber uniformly ($\bar{b} = 0$), there is a net energy transfer from the bunch to the cloud's electrons. However, this energy transfer becomes negligible if the cloud forms a very thin layer at the outer vertical wall ($\bar{b} \simeq 1$). Second, maximum energy transfer occurs when the cloud fills 60% of the beam-chamber in which case the *average* energy gained by an electron ($N_e = 10^{10}$) is less than 1.5eV – this is two orders of magnitude smaller than the regime where the peak of secondary emission makes multi-pactoring a relevant mechanism. Thirdly, note the drastic change in energy in case $\bar{b} = 0.5$. It hints of a significant force when the cloud-vacuum boundary is in the vicinity of the bunch.

A rough estimate of the change in average life-time due to this kick may be performed by observing that the effective energy of the electrons in the cloud increases by E_{kick}. Consequently, assuming that the cloud "remembers" N_{m} out of the N_{b} bunches one is tempted to generalize (8) to read

$$\tau\left(\langle E\rangle\right) \to \tau\left(\langle E\rangle + N_{\mathrm{m}} E_{\mathrm{kick}}\right). \qquad (12)$$

Although simple, the drawbacks of this rough estimate are that it becomes difficult to asses a realistic value of N_{m} and even more important, there is no difference between electrons and positrons bunches.

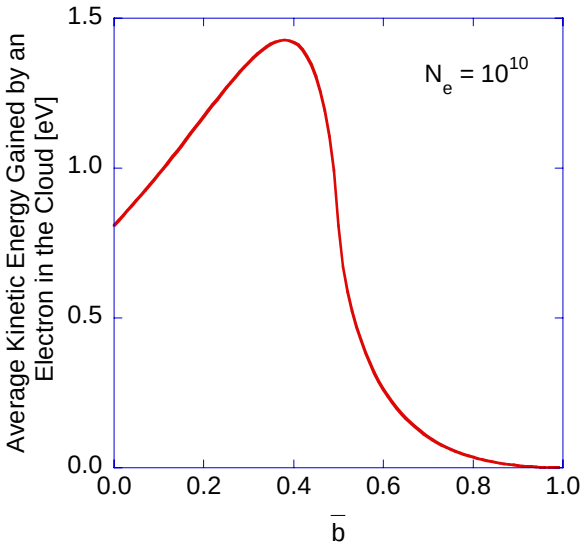

Figure 4: Average kinetic energy gained (E_{kick}) by an electron in the cloud as a function of the cloud's geometric parameter $\bar{b}$.

The next step is to determine the impact of this kick on the life-time of the e-cloud in a more rigorous way. At KEK this was measured [4] to be in excess of 200nsec whereas by examining the vertical tune measurements at CESR, it is possible to conclude that the cloud reaches

equilibrium on a time scale of more than 100-150nsec. For this purpose consider a train with a spacing T between the bunches and let us follow the trajectory of a typical electron in the cloud.

Envision an electron that, after being hit by bunch $\nu-1$, is located at $\left[\delta y_i(0), \delta \dot{y}_i(0)\right]$ in the vertical phase-space. According to (6) and denoting $\psi = \Omega_p t$, its trajectory until bunch ν arrives is given by

$$\begin{pmatrix} \delta y_i(t) \\ \delta \dot{y}_i(t) \end{pmatrix} = \begin{bmatrix} \cosh\psi & \Omega_p^{-1}\sinh\psi \\ \Omega_p \sinh\psi & \cosh\psi \end{bmatrix} \begin{pmatrix} \delta y_i(0) \\ \delta \dot{y}_i(0) \end{pmatrix} \quad (13)$$

whereas based on (9) the impact of a kick changes the momentum of the electron at the moment of impact thus the state-vector varies according to

$$\begin{pmatrix} \delta y_i(t=T+0) \\ \delta \dot{y}_i(t=T+0) \end{pmatrix} = \begin{bmatrix} 1 & 0 \\ -\Omega_{K,\nu} & 1 \end{bmatrix} \begin{pmatrix} \delta y_i(t=T-0) \\ \delta \dot{y}_i(t=T-0) \end{pmatrix}. \quad (14)$$

In the framework of the process described by these equations, the question is whether the *unstable* trajectory of the electrons under the effect of the electron cloud alone, may become *stable* when combining the effect of the attracting force of the positrons? The answer is affirmative but before demonstrating this analytically let us envision the qualitative picture.

Without loss of generality, we consider an electron that after the bunch has passed, is located below the symmetry axis ($y = D_y/2$) moving upwards – see Figure 5. As the next bunch of positrons reaches, it may reverse its direction of motion and force it to move downwards. Similarly, the next bunch may again reverse the trajectory of the electron.

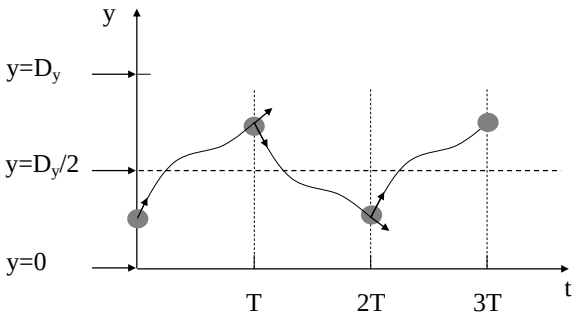

Figure 5: Schematic of the electron's trajectory. The bunches kick the electron with a periodicity T corresponding to the bunch-spacing.

Consequently, according to this simple scenario, the trajectory of the electron may become stable (oscillatory) relative to the symmetry axis ($y = D_y/2$) for the entire duration of the train. Obviously, the periodicity of the motion may be one or more periods of the bunch spacing. It is also important to re-emphasize that the bunch size is assumed to be negligibly small (point-charge) and the oscillations occur on the time scale of the bunch periodicity -- not on the time scale of the bunch duration.

Having this qualitative picture in mind, the next step is to establish the analytic condition for this process to occur. For this purpose, it is necessary to determine the eigen-frequency associated with such a transition of the electron namely,

$$\begin{bmatrix} \cosh(\Omega_p T) & \Omega_p^{-1}\sinh(\Omega_p T) \\ \Omega_p \sinh(\Omega_p T) & \cosh(\Omega_p T) \end{bmatrix} \begin{bmatrix} 1 & 0 \\ -\Omega_{K,\nu} & 1 \end{bmatrix} = e^{j\omega T} \begin{bmatrix} 1 & 0 \\ 0 & 1 \end{bmatrix}. \quad (15)$$

From this eigen-value formulation it is readily concluded that the phase shift ωT during each period is

$$\cos(\omega T) = \cosh(\Omega_p T) - (\Omega_{K,\nu}/2\Omega_p)\sinh(\Omega_p T) \quad (16)$$

and obviously, for a solution, it is necessary to have the right hand side smaller than 1 and larger than -1 implying that

$$2\Omega_p T \tanh(\Omega_p T/2) < \Omega_{K,\nu} T < \frac{2\Omega_p T}{\tanh(\Omega_p T/2)}. \quad (17)$$

This expression relates between the bunch spacing (T), the plasma frequency of the cloud (Ω_P) and the kick frequency (Ω_K) in order to determine whether electron trapping is possible. Clearly there is no stable solution (trapping) if the bunch consists of *electrons* $(\Omega_{K,\nu} < 0)$, since the left hand side can not be satisfied. The condition expressed in (17) is depicted in Figure 6.

It should be pointed out that the bunch spacing (T) may be conceived as a *scaling-parameter* of the trapping process. From Figure 6 we conclude that for high values of the normalized plasma frequency ($\Omega_p T$) and the normalized kick-frequency ($\Omega_K T$) the constraint for trapping becomes very stringent. However, for relatively low values this constraint becomes less severe.

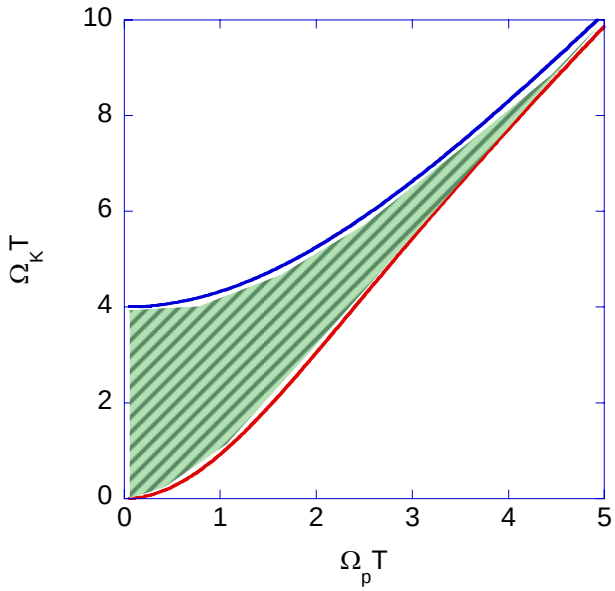

Figure 6: Range of possible solution of (16). At low values the trapping is possible and it becomes more difficult for high values of $\Omega_p T$ and $\Omega_K T$.

After demonstrating the feasibility of electrons becoming trapped in the vertical direction, the remaining question is what fraction of the new-born electrons are being trapped. In order to answer this question, it is convenient to normalize the variables that determine the electrons' vertical phase-space. According to (13)-(14) it is evident that the natural choice is $\bar{y}_1 = 2\delta y / D_y$ and $\bar{y}_2 = 2\delta \dot{y} / D_y \Omega_p$. With this notation the condition that the electrons are confined inside the beam-chamber is $|\bar{y}_1| < 1$ whereas the fact that the trapped electrons undergo a periodic trajectory entails $\bar{y}_1^2 + \bar{y}_2^2 \le 1$. The left-frame of Figure 7 illustrates a uniform phase-space distribution at some initial time and in the right-frame the remaining electrons which satisfy the two trapping conditions mentioned above. Explicitly this can be expressed as

$$E \le E_p \left[1 - \bar{y}_1^2\right] \le E_p \equiv E_{\max,\mathrm{ps}} . \qquad (18)$$

In the context of the dynamics between two bunches, e.g. (7), this entails that only electrons that *bounce back* to the initial electrode are candidates for trapping whereas electrons that have enough energy to overcome the potential barrier associated with the space-charge of the cloud, they will not be trapped. At this point, it is possible to evaluate the average life-time of an electron which started as a "new-born" and at a certain moment it was trapped by the train of *positron bunches*. While exact evaluation of the life-time of a trapped electron in a train of N_b positron bunches is in principle possible, we limit our discussion to a less rigorous estimate.

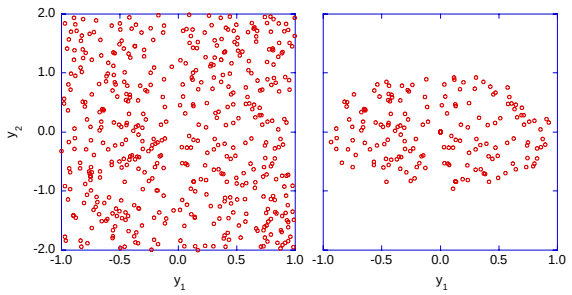

Figure 7: Left-frame illustrates a possible phase-space of new-born electrons whereas the right-frame shows the fraction of this phase-space that corresponds to trapped electrons.

Since in *average*, such a trapped electron sees $N_b / 2$ bunches, and only a fraction of the phase-space corresponds to trapped electrons, we conclude that the life time is

$$\tau = \int_0^{E_p} dE \left(\frac{1}{2} N_b T \right) f_{\mathrm{ec}}^{(\mathrm{p})}(E) + \int_{E_p}^{\infty} dE\, \tau'(E)\, f_{\mathrm{ec}}^{(\mathrm{p})}(E) . \qquad (19)$$

Clearly, the first term represents the contribution to the life-time of trapped electrons whereas the second determines the contribution of the un-trapped ones. Repeating this logic, we may conclude that in case of a train of *electron bunches*, since no trapping is possible, the average life-time of the cloud is

$$\tau = \int_0^{\infty} dE\, \tau'(E) f_{\mathrm{ec}}^{(\mathrm{e})}(E) . \qquad (20)$$

Note that the superscript in the two distribution functions emphasizes that the electrons spectrum in case of a positrons train (superscript – p) is different than in case the train consists of electrons (superscript – e) due to attraction or repulsion correspondingly.

These two expressions reflect two important results of this study. The difference between the impact of a train of positron bunches comparing to a train of electron bunches, from the perspective of the cloud, is not simply because the latter repels the electrons whereas the former attracts them, but rather the train of positrons can actually resonantly trap electrons, virtually for its entire duration. Trapping not only directly extends the life-time of the cloud, but as emphasized when describing the build-up process, it causes an increased average density of the cloud – see (2).

In case of uniform distribution of electrons in the range $0 < E < E_0$ life-time in case of positrons bunches is

$$\tau = \frac{1}{E_0 - E_p} \int_{E_p}^{E_0} dE\, \tau'(E) \left(1 - \frac{E_p}{E_0}\right) + \frac{1}{2} NT \frac{E_p}{E_0} \qquad (21)$$

whereas in case of electron bunches it reads

$$\tau = \frac{1}{E_0} \int_0^{E_0} dE\, \tau'(E) . \qquad (22)$$

VERTICAL TUNE

At this stage we are in position to utilize the tools developed so far for establishing the quasi-static contribution of the EC to the vertical tune. For this purpose, rather than dealing with each component of the lattice separately, the explicit assumption of the model is that from the perspective of an individual bunch the cloud is uniform along the circumference of the ring. In other words, if in practice a bunch experiences a cloud which is a periodic function of the coordinate s namely, $n_{\mathrm{ec}}(s) = \sum_{n=-\infty}^{\infty} n_{\mathrm{ec},n} \exp\left(j 2\pi n s / C\right)$, then in the framework of the present model, only the zero harmonic is considered. This does not mean that all the bunches experience the same e-cloud, in fact, the opposite is at the essence of the present analysis – see Eq. (4).

If exactly on axis, symmetry of the cloud entails zero vertical force on either positron ($+e$) or electrons ($-e$) bunch; however, if the positron bunch is displaced off axis by δy the cloud exerts a vertical attracting force $+eE_y$ and in Appendix C it is demonstrated that

$$\frac{+eE_y}{mc^2\gamma} = \frac{\delta y}{\beta_{\mathrm{ec}}^2} \quad , \quad \frac{1}{\beta_{\mathrm{ec}}^2} = \frac{-e}{m_0 c^2 \gamma} \frac{n_{\mathrm{ec},0} D_x}{4\pi\varepsilon_0} \frac{f_E\left(\bar{b}\right)}{D_y} \qquad (23)$$

β_{ec} has units of length and it may be interpreted as the beta-function associated with a stationary electron-cloud

[8]; in the same appendix the explicit expression for the form-factor $f_E(\bar{b})$ is developed. With the expression in (23) the vertical motion of the positron bunch may be described by

$$\left[\frac{d^2}{ds^2}+\frac{1}{\beta_y^2}\right]\delta y=\frac{1}{\beta_{\rm ec}^2}\delta y \qquad (24)$$

entailing an effective beta-function $\beta^{-1}\equiv\sqrt{\beta_y^{-2}-\beta_{\rm ec}^{-2}}$ and thus, the vertical tune being given by

$$Q_y=\frac{1}{2\pi}\oint\frac{ds}{\beta}\simeq\frac{1}{2\pi}\left[\oint\frac{ds}{\beta_y}-\oint\frac{ds\beta_y}{2\beta_{ec}^2}\right] \qquad (25)$$

tacitly assuming that the tune-shift due to the EC effect is small. With this observation in mind, clearly the *relative* tune-shift of a bunch is proportional to the *cloud density* it experiences. Moreover, since in the framework of this model it is assumed that from the perspective of the bunch this cloud is uniform in the longitudinal direction, we conclude that

$$\delta Q[\%]=100\times\frac{Q_y-Q_y^{(0)}}{Q_y^{(0)}}\simeq 50\frac{\beta_c^2 r_e}{\gamma}\frac{D_x}{D_y}f_E\left(\bar{b}\right)n_{\rm ec} \qquad (26)$$

wherein the coupling beta function is a coefficient determined by the lattice properties and for CESR at 2GeV

$$\beta_c^2\equiv\frac{\oint ds\beta_y(s)}{\oint ds\frac{1}{\beta_y(s)}}\simeq\begin{cases}240.8\left[\mathrm{m}^2\right] & 12\,\text{wigglers}\\ 252.4\,[\mathrm{m}^2] & 6\,\text{wigglers}\end{cases} \qquad (27)$$

For completeness it warrants to indicate that a similar procedure may be adopted for evaluating the horizontal tune-shift with one major difference. With the exception of the case when the cloud fills uniformly the entire volume, the cloud exerts a horizontal force on the bunch even when it is exactly on axis. This force can be assumed to be compensated by the lattice. In Appendix C it is shown that the horizontal tune-shift is *negative* if the cloud fills less than half of the volume $(\bar{b}\geq 0.5)$ namely, when the bunches move in vacuum. At the other extreme, when the electron cloud fills the entire beam-chamber $(\bar{b}\sim 0)$ and the bunch passes through the cloud, the horizontal tune-shift is *positive* and it may become significantly smaller than the vertical tune-shift.

OPTIMIZATION PROCEDURE

As indicated in (4), in case of a train of bunches, each bunch experiences a different density and therefore, combining this result with the one in (26) the relative tune shift may be formulated as

$$\delta Q_\mu[\%]\simeq\bar{q}\sum_{\nu=1}^{N_b}W_{\mu,\nu}\exp\left[-(\mu-\nu)T/\tau\right] \qquad (28)$$

wherein

$$\bar{q}\equiv 50\frac{\beta_c^2 r_e}{\gamma}\frac{D_x}{D_y}f_E\left(\bar{b}\right)n_{\rm nb},\ W_{\mu,\nu}=\frac{I_\nu}{\langle I\rangle}h(\mu-\nu-0) \qquad (29)$$

and $n_{\rm nb}\equiv\left\langle n_\mu^{(\rm nb)}\right\rangle$, revealing that this model consists of two explicit parameters, $\bar{q}$ and τ facilitating to quantify the relative tune shift experienced by the various bunches. To be more accurate $\bar{q}$ is determined by the average density of new-born electrons $n_{\rm nb}$ and the cloud geometry (b) whereas the life-time (τ) depends in addition to these two on the train duration $\left(N_b\right)$ as well as on the average initial energy of the new-born electrons $\left(\langle E\rangle\right)$. Based on the *experimental* data it is possible to deduce the values of these two parameters of the model $\left(\bar{q},\theta\equiv T/\tau\right)$ out of the three unknown parameters of the cloud $\left(n_{\rm nb},b,\langle E\rangle\right)$.

For establishing these two parameters from the experimental data we pursue a standard optimization procedure. Defining, based on (28), the function $G_\mu(\theta)\equiv N_b\left\langle W_{\mu,\nu}\exp\left[-\theta(\mu-\nu)\right]\right\rangle_\nu$ as well as the function which evaluates the error $\mathrm{Error}(\bar{q},\theta)=\left\langle\left[\delta Q_\mu^{(\rm exp)}-\bar{q}\,G_\mu(\theta)\right]^2\right\rangle_\mu$, it is possible to establish the optimal $\bar{q}$ for a given θ. The result,

$$\bar{q}_{opt}(\theta)=\left\langle\delta Q_\mu^{(\rm exp)}G_\mu(\theta)\right\rangle_\mu\left\langle G_\mu^2(\theta)\right\rangle_\mu^{-1} \qquad (30)$$

is substituted in the "error-function". At this stage, it becomes natural to redefine the error-function for the life-time parameter alone therefore the relative error is

$$\mathrm{Error}_{\rm n}(\theta)=100\times\left[1-\frac{\left\langle\delta Q_\mu^{(\rm exp)}G_\mu(\theta)\right\rangle_\mu^2}{\left\langle G_\mu^2(\theta)\right\rangle_\mu\left\langle\left[\delta Q_\mu^{(\rm exp)}\right]^2\right\rangle_\mu}\right] \qquad (31)$$

Obviously, the outcome of this optimization procedure are the two parameters $\bar{q}_{opt},\theta_{opt}$ and the relative error $\varepsilon=\mathrm{Error}_{\rm n}\left(\theta_{opt}\right)$.

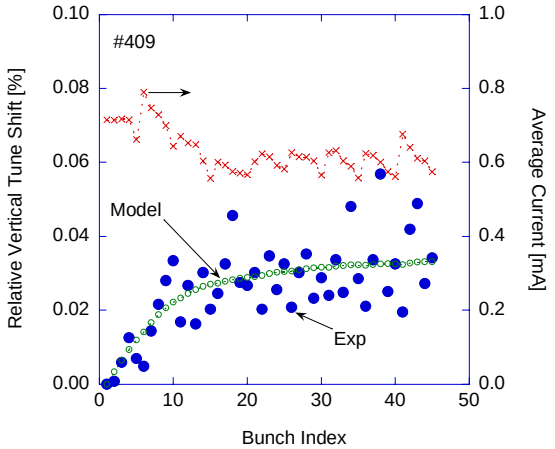

Figure 8: The experimental data (blue-solid circle) and the model results (green circle) corresponding to: $\theta_{opt}=0.09$, $\varepsilon=7.7\%$ and $\bar{q}_{opt}=3.28\times10^{-3}$. The average current of each bunch is marked with red-x and it should be read on the right scale; the experimental data was taken on September 6, 2006.

Figure 8 illustrates the experimental data and the model results which are the outcome of the optimization; $\theta_{opt} = 0.09$, 7.7%, $\bar{q}_{opt} = 3.28\times10^{-3}$ the average current of a bunch is 0.63[mA] corresponding to about 10^{10} electrons in average in each bunch. The immediate result of this optimization is evident: the life time of the cloud is of the order of 155nsec (T=14nsec). The fluctuations of the experimental data around the values predicted by this quasi-static model may be attributed to the wake generated by the bunch in the cloud and its effect back on the bunches – description of this mechanism is beyond the scope of this study.

With these optimal parameters established, let us determine the constraints that will enable to determine the cloud parameters. Relying on the definition of $\bar{q}$ in (29) we realize that

$$f_E\left(\bar{b}\right) n_{\rm nb} = 2\times10^{11}\left[m^{-3}\right] \qquad (32)$$

This may be further simplified recalling that when describing the build-up process it was shown that for a sufficiently long train equilibrium is reached after a typical time τ and the equilibrium entails $n_{ec} \simeq n_{nb}\tau / T$ hence

$$n_{\rm ec}\left[m^{-3}\right] = \frac{2.22\times10^{12}}{f_E\left(\bar{b}\right)} = \frac{n_0}{f_E\left(\bar{b}\right)}. \qquad (33)$$

The second constraint results from the optimization of the life-time. Ignoring momentarily the effect of the *train* on the life-time (trapping) this expression entails

$$\frac{1}{0.09} = \frac{2}{\Omega_p T} g\left(2\frac{\langle E\rangle}{E_p}\right). \qquad (34)$$

Combining the two equations we get

$$\frac{f_P\left(\bar{b}\right)}{f_E\left(\bar{b}\right)} = 0.023 g^2\left(0.16\langle E\left[eV\right]\rangle \frac{f_E\left(\bar{b}\right)}{f_P\left(\bar{b}\right)}\right) \qquad (35)$$

which has *no solution* for any *b* and *E*. However, including the effect of the train we find that

$$\frac{\tau}{T} = \frac{1}{0.09} = \frac{2}{\Omega_p T} g\left(2\frac{\langle E\rangle}{E_p}\right) + \frac{1}{2} N_b \frac{E_p}{2\langle E\rangle} \qquad (36)$$

and as demonstrated next, (36) and (33) do have a self-consistent solution.

Using the definitions of Ω_p, E_p and the expression in (33) may be rewritten as $E_p\left[eV\right] = 12.54\, f_P\left(\bar{b}\right) / f_E\left(\bar{b}\right)$ or $\Omega_p T = 1.176\sqrt{f_P\left(\bar{b}\right) / f_E\left(\bar{b}\right)}$. These two representations are then substituted in (36) and for a given average energy of the new-born electrons $\left(\langle E\rangle\right)$ there is a solution for the resulting equation in terms of a resulting cloud geometry $\left(\bar{b}\right)$ as illustrated in the top frame of Figure 9.

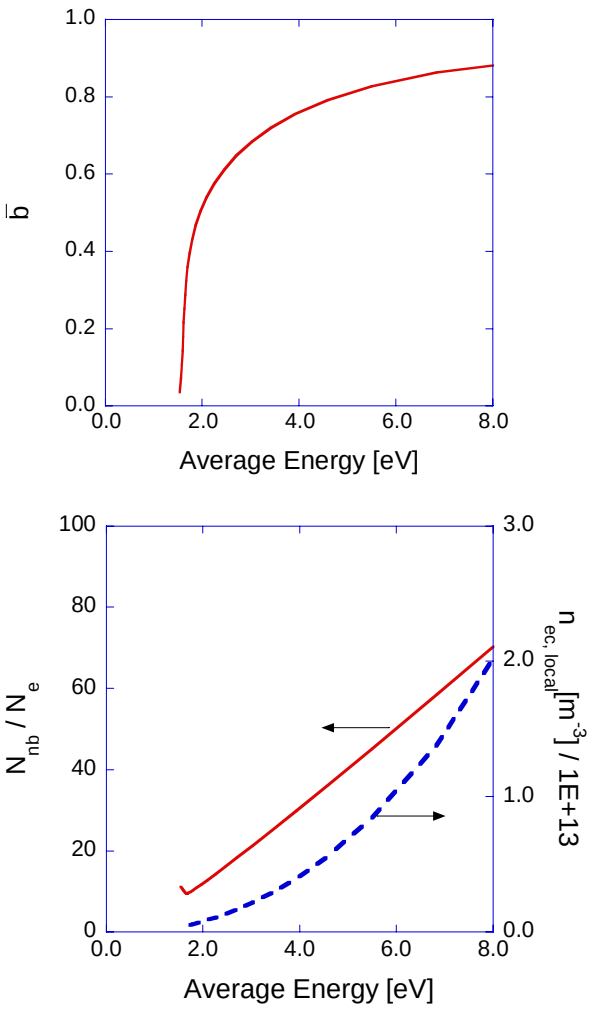

Figure 9: *Top frame*. Cloud formation as a function of the average energy of the electrons consisting the electron cloud. *Bottom frame*. The number of "new-born" electrons whatever the mechanism is increases linearly with their initial energy. Local density of the cloud increases almost quadratically with the energy.

In its top-frame, Figure 9 reveals that according to the parameters of the experiment, at low average energy of the new-born electrons no cloud is formed. However, beyond 1eV the cloud forms and it is roughly uniform across the beam-chamber. If the average energy of the new-born electrons is increased, then the cloud shrinks in size and it is all concentrated near the outer wall of the ring. In this process, the local density in the cloud increases almost quadratically with the energy – see bottom frame. This frame also demonstrates that the number of new-born electrons whatever the mechanism is (photo-electrons, secondary-electrons, stray electrons or ionization electrons) increases linearly with their *average* energy.

It is instructive at this stage to go back to the second section where we discussed the build-up process. In a set of runs performed on April 2nd 2007 at CESR, a split train of positron bunches was considered. Figure 10 shows three representative results (red squares) and in parallel the model was used to determine the ability to have a good fit of the experimental data. The top frame (#2081) clearly shows what was indicated in the context of (3) namely, that when the life-time is much longer than the bunch-spacing, then the build-up is independent on the former -- $\delta Q_\nu \propto n_{ec,\nu} = n_{nb}\nu$; in the optimization process this independence reflected in large variations in θ_{opt} without significant impact on the relative error.

Injecting a secondary train of five bunches (middle frame, #2085) allows to determine properly the life-time. It is clearly observed that due to the exponential decay the cloud density (represented here by the vertical tune shift) is significantly smaller than that experienced by bunch #10. In fact, the main contribution to the relative error comes from the this bunch. For a better fit of its value the life-time should have been increased but this would have increased the error associated with the bunches in the secondary train. Note that the last bunches in the secondary train experience the cloud generated by their preceding counterparts. This fact is even better revealed in the bottom-frame (#2093) where the secondary train is more packed (14,15,16,17,18) and much closer to the first train.

In principle, bearing in mind that it is possible to asses the spectrum of the electrons experimentally, we could conclude the analytic model at this stage. However, this information is not available as yet, nevertheless, in order to gain some partial insight regarding the relative weight of two of the processes namely, photo-emission and secondary emission, we ignore in what follows the other two.

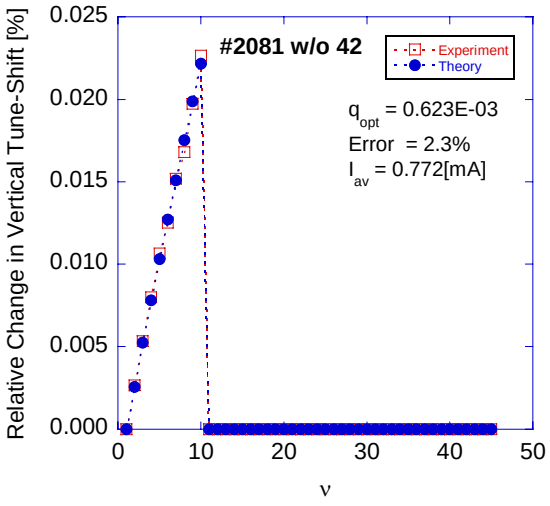

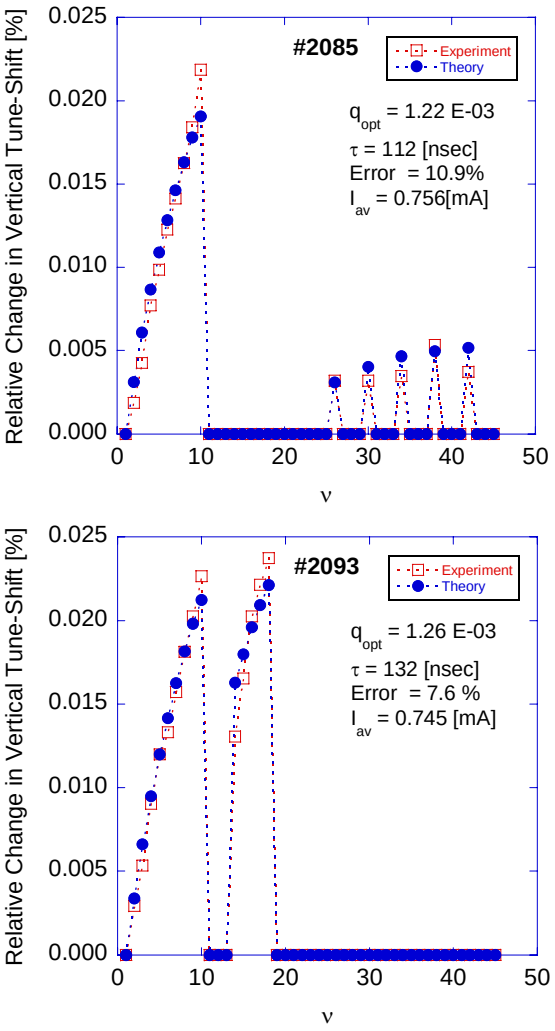

Figure 10: Relative change in the vertical tune-shift as experienced by each bunch (index ν). Top frame shows very good agreement between the experimental data (red squares) and the best-fit based on the theoretical model (blue diamonds) when only the firs section of the train were injected (bunches 1-10). Since the bunch life-time is much longer than the bunch spacing (14nsec) the build-up is only a function of the latter. In the middle frame, the train was split into two parts: the first section was identical but in the second, bunches 26, 30, 34, 38 and 42 were also injected. According to the best fit model, the life-time is 112nsec. While the error of the fit is reasonable its main component is from bunch #10. In the last frame the only change relative to the middle frame is the bunches injected: 14, 15,16,17 and 18; the corresponding life-time was calculated to be 132nsec.

PHOTO-ELECTRONS

First it is demonstrated that *photo-electrons alone* can not account for all the new-born electrons. In order to justify this statement we pursue the following approach: the number of photons generated by N_e electrons (or positrons) is

$$\frac{N_{\rm ph}}{N_e} \simeq 130 \times E_k[GeV] \qquad (37)$$

Similarly, the number of photo-electrons generated is

$$\frac{\bar{N}_{\rm pe}}{N_e} = 130 \times E_k[GeV]\ \bar{\delta}_{\rm pe} \qquad (38)$$

where $\bar{\delta}_{\rm pe}$ is the integrated photo-electrons yield - see Appendix D. Relying on studies by Groebner [9] ignoring reflections and assuming Aluminium we calculated the average yield to be $\bar{\delta}_{\rm pe} \simeq 0.1$. This is an overestimate since it is tacitly assumed that all the photo-electrons generated on the outer-vertical wall can penetrate the magnetic field lines. Nevertheless, this rough estimate is adopted since it enables to pursue a relatively simple model for the spectrum of the photo-electrons which can be approximated ($E_{\rm cr} \gg E_{\rm w}$) by

$$f_{\rm pe}(E) \simeq \frac{4}{E_{\rm cr}} \begin{cases} 1 & E < E_{\rm w} \\ \exp\left(-4\dfrac{E-E_{\rm w}}{E_{\rm cr}}\right) & E > E_{\rm w} \end{cases} \qquad (39)$$

$E_{\rm w} \simeq 4[eV]$ is the work function of Aluminium and $E_{\rm cr} = 3\gamma^3 c\hbar/\rho \simeq 444[eV]$ at 2GeV; $\rho = 80[m]$. Consider now the number of photo-electrons of energy between zero and E_0

$$\begin{aligned} N_{\rm pe}(E_0) &= 130 \times E_k[GeV]\ \bar{\delta}_{\rm pe} N_e \int_0^{E_0} dE\, f_{\rm pe}(E) \\ &\simeq 130 \times E_k[GeV]\ \bar{\delta}_{\rm pe} N_e \frac{4E_0}{E_{\rm cr}} \end{aligned} \qquad (40)$$

and their corresponding average energy is

$$\langle E \rangle_{\rm pe} = \frac{\int_0^{E_0} dE\, E\, f_{\rm pe}(E)}{\int_0^{E_0} dE\, f_{\rm pe}(E)} \simeq \frac{1}{2} E_0 \,. \qquad (41)$$

For example, if $\langle E \rangle \sim 2[eV]$ the photo-electrons may account for roughly one,

$$\frac{N_{\rm pe}}{N_e} = 130 \times E_k[GeV] \bar{\delta}_{\rm pe} \left(8\frac{\langle E \rangle_{\rm pe}}{E_{\rm cr}}\right) \sim 1 \qquad (42)$$

out of 15 new-born electrons. Obviously, if the stray electrons and the ionization electrons are ignored, the secondary electrons should account for the remainder and they will be considered next.

SECONDARY ELECTRONS

For examining the impact of secondary electrons consider a differential yield $\delta_{\rm se}(E, E')$ such that the probability-density of emitting a secondary electron is given by

$$f_{\rm se}(E) = \int_0^{\infty} dE'\, \delta_{\rm se}(E, E')\, f_{\rm pe}(E') \,. \qquad (43)$$

This simplifies by assuming that each incoming electron generates a given distribution of true-secondary electrons (subscript ts) [10]

$$f_{\rm ts}(E, \varepsilon, p, E') = \frac{(E/\varepsilon)^{p-1}}{\varepsilon \Gamma(p)} \exp\left(-\frac{E}{\varepsilon}\right) h(E'-E) \qquad (44)$$

ε, p are two parameters of the material. Note that $\int_0^{\infty} dE\ f_{\rm ts} = 1$ and $\int_0^{\infty} dE E\ f_{\rm ts} = \varepsilon p$ -- assuming that the energy of the incoming electron is larger than the characteristic energy ε; the step-function in (44) takes care of the fact that the energy of the emerging electrons is limited by the energy of the incoming electron. Secondary electrons which are result of elastic scattering are ignored. Further, we use the secondary emission yield [11]

$$\begin{aligned} \tilde{\delta}_{\rm se}(E') &= \delta_{\max} \frac{1}{g_n(z_{\rm m})} g_n\left(z_{\rm m} \frac{E}{E_{\max}}\right) \\ g_n(z) &= \left[1 - \exp\left(-z^{n+1}\right)\right] z^{-n} \end{aligned} \qquad (45)$$

where the typical values are $n \simeq 0.35$, $z_m \simeq 1.84$ wherein $\delta_{\max}$ is the value of maximum yield and $E_{\max} \sim 300[eV]$ is the energy where it occurs. With these definitions, the probability-density reads

$$f_{\rm se}(E) = f_{\rm ts}(E) \int_E^{\infty} dE'\, \tilde{\delta}_{\rm se}(E')\, f_{\rm pe}(E') \qquad (46)$$

and thus, the number of secondary-electrons generated in the range between $0 \div E_0$ is

$$N_{\rm se}(E_0) = 130 \times E_k[GeV]\ \bar{\delta}_{\rm pe} N_e \int_0^{E_0} dE\, f_{\rm se}(E) \,. \qquad (47)$$

Being an integral quantity, this number may be larger than the number of photo-electrons (40) although the energy range does not cover the range of maximum secondary yield.

With (46) in mind, in the same range ($0 \div E_0$), the average energy of the secondary electrons is

$$\langle E \rangle_{\rm se} = \frac{\int_0^{E_0} dE\, E\, f_{\rm se}(E)}{\int_0^{E_0} dE\, f_{\rm se}(E)} \,. \qquad (48)$$

Evidently, the total number of electrons is $N_{\rm pe+se}(E_0) = N_{\rm pe}(E_0) + N_{\rm se}(E_0)$ implying that the ensemble average energy of the electrons in the energy range specified above is

$$\langle E \rangle = \langle E \rangle_{\rm pe} \frac{N_{\rm pe}}{N_{\rm pe} + N_{\rm se}} + \langle E \rangle_{\rm se} \frac{N_{\rm se}}{N_{\rm pe} + N_{\rm se}} \,. \qquad (49)$$

Figure 11 illustrates the number of new-born electrons as predicted by the model base on the experimental data (right frame of Figure 9) indicating linear dependence on the average energy at (relatively) high energies. This is compared with the (over-simplified) picture developed in the last two sections, including photo-electrons and secondary-electrons alone, revealing a reasonable close value for $\delta_{\max} \simeq 1.8$, $p = 2$ and $\varepsilon = 2[eV]$ -- blue curve. It should be pointed out that we do not know the parameters ε and p for Aluminium however, in Ref. 10 the authors provide these numbers for copper and stainless steel. We chose these two parameters to be

reasonably close to the parameters of copper ($p = 2.09 \pm 0.67$ and $\varepsilon \simeq 3.9 \pm 3.2$). The maximum $\delta_{\max}$ was a result of an optimization process attempting to minimize the absolute difference between the data points of the two curves. While the behaviour of the two curves is quite different the order of magnitude is fairly close implying that the photo-electrons and the secondary electrons play a central role. At the same time, the difference between the two curves is sufficient to hint that the other two contributions (ionization and stray-electrons) are not negligible.

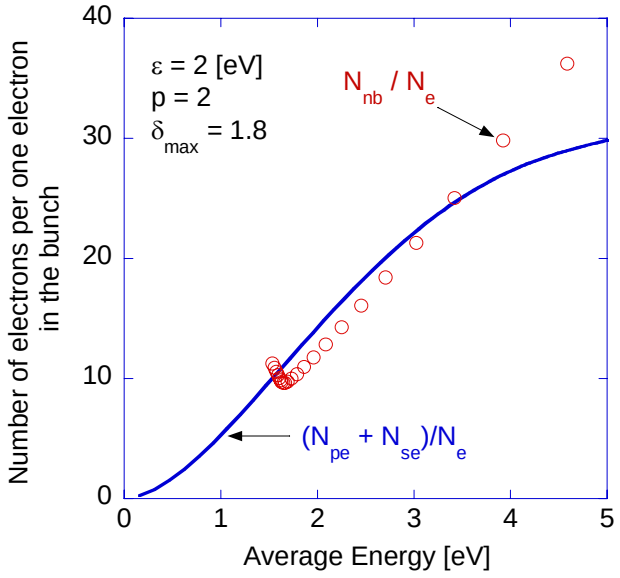

Figure 11: Relative number of new-born electrons as a function of their average energy based on both the model and the "experimental" data (red-circles) and the average number of photo and secondary electrons (per electron in the bunch) as a function of their average energy.

It was demonstrated in the previous section that the photo-emission may account for one out of about 15 electrons in the cloud. For a better assessment the relative weight between the two species, it is convenient to define the *integrated* secondary emission yield as the ratio of total number of secondary electrons and the total number of photo-electrons in the energy range of relevance namely, $N_{\mathrm{se}}(E_0)/N_{\mathrm{pe}}(E_0)$. The two quantities are defined in (47) and (40) correspondingly and E_0 is the upper limit of the energy range of interest. Two facts are revealed by the red-curve in Figure 12: first, the ratio of the two populations is indeed of the order of 15. This peak occurs at an ensemble average energy 2eV. Second, this ratio is dominated by the *spectrum* of "true-secondaries" – defined in (44) and normalized here such that the peak value is unity (blue-curve). With this regard, the horizontal variable should be interpreted as energy of emerging secondary electron rather than ensemble average in the case of the integrated secondary emission yield.

This last result should be very cautiously interpreted since the assumption made, whereby ionization electrons are neglected seems to pose a very stringent constraint. Moreover, lack of exact knowledge regarding the values of the two parameters that describe the spectrum of "true-secondary" electrons (ε, p) oblige us to interpret the results of this section as a general *trend* at the most. Albeit we believe that the role of low energy secondary electrons and their specific spectrum is of great importance to the overall equilibrium of the electron cloud.

Before concluding it warrants to re-emphasize that the beam-chamber in CESR is made out of Aluminium and we can not rule out that locally, a thin layer of Al_2O_3 covers the wall and locally there might be enhanced secondary emission [12]. In the framework of this model we can not resolve such enhanced emission spots but it may manifest itself as an enhanced global secondary emission yield.

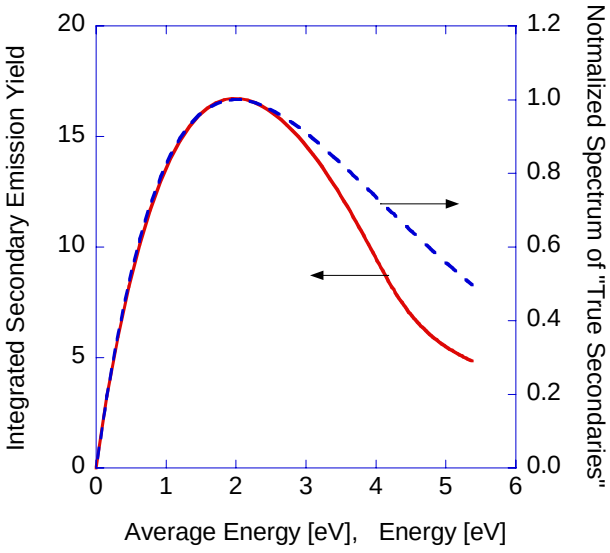

Figure 12: The integrated secondary emission yield (red-solid curve) as a function of the ensemble average energy (Eq.(49)). Spectrum of the "true-secondary" electrons normalized to its maximum value. At low energies both curves have a virtually identical trend.

SUMMARY AND DISCUSSION

The essence of the model developed here is to examine the electron cloud from the perspective of each bunch separately since each bunch experiences a different cloud density according to its location in the train. It has been pointed out that the average life-time of the electrons in the cloud is a crucial parameter which, together with the "new-born" electrons density and the bunch spacing, determine the average density of electrons – see (2).

Determining the cloud density *as experienced by each bunch* is essential for establishing the tune-shift of each bunch. For example, it is obvious that there is no tune-shift for the first bunch in the train since the cloud it generates may affect only trailing bunches therefore it was natural to refer all the changes to that of the first one. Moreover, according to the life-time of the cloud, there is a build-up process that encompasses a number of bunches ($N_{\text{build-up}}$) such that the build-up duration corresponds to the typical life-time namely, $N_{\text{build-up}}T \sim \tau$. After this build-up time, the system reaches equilibrium determined quantitatively by the expression in (2). Excellent agreement between the experimental data and the model predictions regarding the build-up were revealed in Fig. 10 .

An important process that affects the life-time is the *vertical trapping* of slow electrons by a train of positron bunches. This process may alter significantly the average life-time of the cloud. Nevertheless, even in the absence of trapping it was demonstrated that the life-time may exceed 200[nsec]. However, for the CESR September 2006 results, without accounting for the trapping, this model could not account for the measured vertical tune-shift.

According to the present model the typical energy of the electrons in the cloud is a *few* electron-volts. In addition, only the direct kick due to the bunch self-field was considered, ignoring the possible effect of the wake trailing behind each bunch. Subject to this assumption, it has been demonstrated that in average, an electron in the cloud may gain less than 2[eV]. Together with the initial average energy of an electron in the cloud, this is insufficient to sustain multi-pactoring process since according to existing secondary emission models the typical energy where the maximum yield occurs is 300[eV].

Based on the present model and the experimental data from CESR, photo-electrons contribute one out of more than 15 electrons in the cloud for each positron in the bunch thus the remainder should be attributed to either secondary emission, or ionization of the background gas or stray electrons or all three combined. A crude model of the secondary emission was adopted but lack of information of the characteristic parameters of the "true-secondary" electrons spectrum for Aluminium, restricts significantly the validity of the result. Nevertheless, it clearly demonstrates that the spectrum of the low-energy (<6eV) secondary electrons, could dominate the electron cloud.

Finally, although the focus of this study is the vertical tune-shift, the model enabled us to draw an important conclusion regarding the *horizontal* tune-shift. The latter is *negative* if the cloud fills less than half of the volume $(\bar{b} \geq 0.5)$ namely, when the bunches move in vacuum. At the other extreme, when the electron cloud fills the entire beam-chamber $(\bar{b} \sim 0)$ and the bunch passes through the cloud, the horizontal tune-shift is *positive* and it may become significantly smaller than the vertical tune-shift.

ACKNOWLEDGEMENT

For introducing me to the subject I wish to thank Maury Tigner, David Rice and Mark Palmer. Eugene Tanke and Gerry Codner were very helpful elucidating some aspects of the experimental data. James Crittenden has provided me with the data facilitating to evaluate the coupling beta function (27) for CESR. I am grateful to valuable feedback regarding this model from Kathy Harkay and John Flanagan. Discussion with Ilan Ben Zvi regarding secondary emission is also appreciated.

APPENDIX A

In this appendix we determine the life-time of an electron which leaves one of the walls and is subject to an electrostatic potential constraint by the boundary conditions associated with the beam-chamber. The effect of the bunches on the dynamics of the electrons is ignored. Between kicks the dynamics of the electrons is governed by the cloud thus

$$\begin{aligned}\frac{d^2}{dt^2}\delta y_i &= \frac{e}{m}\sum_{n_x,n_y=1}^{\infty}\phi_{n_x,n_y}\left(\frac{\pi n_y}{D_y}\right)\cos\left[\frac{\pi n_y}{D_y}\left(\frac{D_y}{2}+\delta y_i\right)\right] \\ &\times\left\{\frac{1}{1-\bar{b}}\frac{1}{\pi n_x}\left[\cos\left(\pi n_x\bar{b}\right)-\cos\left(\pi n_x\right)\right]\right\} \\ \phi_{n_x,n_y} &= -\frac{en_{local}}{\varepsilon_0}\frac{\frac{8}{\pi^4 n_x n_y}\sin^2\left(\frac{\pi}{2}n_y\right)}{\left(\frac{n_x}{D_x}\right)^2+\left(\frac{n_y}{D_y}\right)^2}\Lambda_{n_x}\left(\bar{b}\right)\end{aligned} \qquad (50)$$

$$\Lambda_{n_x}\left(\bar{b}\right)=\cos\left(\pi n_x\bar{b}\right)-\cos\left(\pi n_x\right)$$

A first order approximation is adopted for the right hand side term leads to

$$\begin{aligned}\frac{d^2}{dt^2}\delta y_i &= \delta y_i\frac{e^2 n_{ec}}{m\varepsilon_0}f_P\left(\bar{b}\right)=\delta y_i\Omega_p^2 \\ f_P\left(\bar{b}\right) &= \frac{\left(2/\pi\right)^3}{\left(1-\bar{b}\right)^2}\frac{D_x}{D_y}\sum_{n_x,n_y=1}^{\infty}\frac{n_y}{n_x^2}\frac{\sin^3\left(\frac{\pi}{2}n_y\right)\Lambda_{n_x}^2}{n_x^2\frac{D_y}{D_x}+n_y^2\frac{D_x}{D_y}}\end{aligned} \qquad (51)$$

Assuming that the electron starts from $\delta y_i = -D_y/2$ with an initial velocity $\sqrt{2E_i/m}$ where E_i is the energy the electron is injected into the gap then its trajectory (6) is described by

$$\delta y_i\left(t\right)=\frac{\sqrt{2E_i/m}}{\Omega_p}\sinh\left(\Omega_p t\right)-\frac{D_y}{2}\cosh\left(\Omega_p t\right) \qquad (52)$$

The time it takes the electron to reach the *upper* plane, $\delta y_i\left(t=\tau_i\right)=D_y/2$, depends on the characteristic (potential) energy of the EC

$$E_p=\frac{1}{2}m\left(\Omega_p D_y/2\right)^2 \tag{53}$$

and it is given by

$$\tau_i=\frac{2}{\Omega_p}\operatorname{atanh}\left(\sqrt{\frac{E_p}{E_i}}\right) \tag{54}$$

provided that the initial (kinetic) energy is greater than the potential energy $\left(E_i>E_p\right)$ associated with the cloud.

The particle may bounce back if at $\delta y<0$ the velocity vanishes namely the time it takes a particle to reach the point of zero vertical velocity is derived from $\sqrt{E_i/E_p}=\tanh\left(\Omega_p\tau_{1/2}\right)$ and the overall time the particle spends the beam-chamber is

$$\tau_i=\frac{2}{\Omega_p}\operatorname{atanh}\left(\sqrt{\frac{E_i}{E_p}}\right). \tag{55}$$

To summarize, the time an electron may spend in the cloud subject to the space-charge force alone is given by

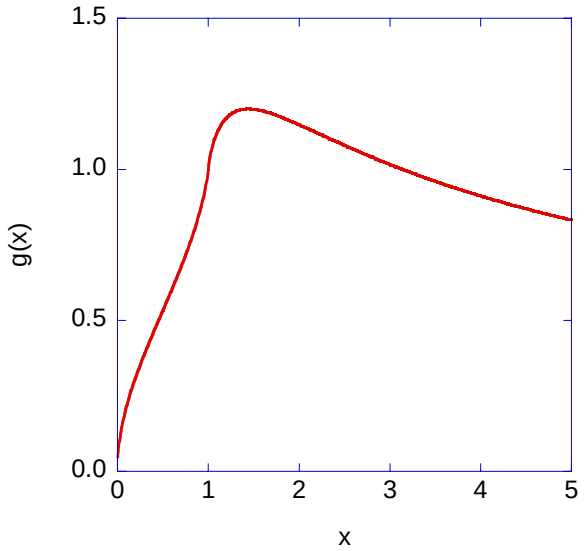

Figure 13: The dependence of the average life-time ($\pi\Omega_p/2$) on the normalized average energy ($x=2\langle E\rangle/E_p$).

$$\tau_i=\frac{2}{\Omega_p}\begin{cases}\operatorname{atanh}\left(\sqrt{E_i/E_p}\right) & E_i<E_p\\ \operatorname{atanh}\left(\sqrt{E_p/E_i}\right) & E_i>E_p\end{cases} \tag{56}$$

For evaluation of the *average* life-time it is assumed that the electron's spectrum is uniform between zero and E_0 implying that the average energy is $\langle E\rangle=E_0/2$ and therefore, the average life-time in terms of the average energy is

$$\tau=\frac{1}{E_0}\int_0^{E_0}dE\,\tau(E)=\frac{2}{\Omega_p}g\left(2\frac{\langle E\rangle}{E_p}\right)$$
$$g(x)=\frac{1}{x}\int_0^x du\begin{cases}\operatorname{atanh}\left(\sqrt{u}\right) & u<1\\ \operatorname{atanh}\left(\sqrt{1/u}\right) & u>1\end{cases} \tag{57}$$

The last function can be evaluated analytically for two regimes of interest ; its exact behaviour is illustrated in the next Figure 13. The maximum of this function occurs for $x_{\max}=1.44$ and its value is $g\left(x_{\max}\right)=1.2$.

APPENDIX B

In this appendix we determine the average kick delivered by a bunch to an electron in the cloud. For this purpose we bear in mind that the potential associated with the train of *positron* bunches is

$$\left[\nabla^2-\frac{1}{c^2}\frac{\partial^2}{\partial t^2}\right]A_z=-\mu_0 V(+e)\sum_{\nu=1}^{N}N_{e,\nu}\delta\left[z-V\left(t-\nu T\right)\right]$$
$$\times\delta\left(x-\frac{D_x}{2}\right)\delta\left(y-\frac{D_y}{2}\right)$$

$$A_z(x,y,z,t)=\sum_{n_x,n_y=1}^{\infty}a_{n_x,n_y}\sin\left(\pi n_x\frac{x}{D_x}\right)\sin\left(\pi n_y\frac{y}{D_y}\right) \tag{58}$$

thus defining $\chi_{n_x,n_y}=\left[\left(\pi n_x/D_x\right)^2+\left(\pi n_y/D_y\right)^2\right]D_xD_y$ and assuming $\gamma\gg1$ we get

$$E_y=-\frac{(+e)}{\varepsilon_0}\sum_{\nu=1}^{N}N_{e,\nu}\delta\left[z-V\left(t-\nu T\right)\right]$$
$$\times\sum_{n_x,n_y=1}^{\infty}\sin\left(\pi n_x\frac{x}{D_x}\right)\left[\frac{d}{dy}\sin\left(\pi n_y\frac{y}{D_y}\right)\right] \tag{59}$$
$$\times\frac{4}{\chi_{n_x,n_y}}\sin\left(\frac{\pi}{2}n_x\right)\sin\left(\frac{\pi}{2}n_y\right)$$

Averaging over the horizontal dimension of the cloud we get

$$\bar{E}_y=\frac{1}{D_x-2b}\int_{D_x-2b}^{D_x}dx E_y$$
$$=-\sum_{\nu=1}^{N}N_{e,\nu}\delta\left[z-V\left(t-\nu T\right)\right]\sum_{n_y=1}^{\infty}\phi_{n_y}^{(b)}\frac{d}{dy}\sin\left(\frac{\pi n_y y}{D_y}\right)$$
$$\phi_{n_y}^{(b)}=\frac{(+e)}{\varepsilon_0}\sin\left(\frac{\pi}{2}n_y\right)\sum_{n_x=1}^{\infty}\frac{4}{\chi_{n_x,n_y}}\sin\left(\frac{\pi}{2}n_x\right)\frac{1}{1-\bar{b}}\frac{\Lambda_{n_x}}{\pi n_x} \tag{60}$$

without loss of generality we assume the kick of the i'th electron is given by

$$\left.\frac{dy_i}{dt}\right|_{t=\nu T-0}^{t=\nu T+0}=\frac{eN_{e,\nu}}{mV}\sum_{n_y=1}^{\infty}\phi_{n_y}^{(b)}\left[\frac{\pi n_y}{D_y}\cos\left(\pi n_y\frac{y_i}{D_y}\right)\right] \tag{61}$$

For a small deviation $y=D_y/2+\delta y$ we get

$$\left.\frac{d\delta y_i}{dt}\right|_{t=\nu T+0} - \left.\frac{d\delta y_i}{dt}\right|_{t=\nu T-0} = -\Omega_{K,\nu}\left(\delta y_i\big|_{t=\nu T}\right) \quad (62)$$

Consequently, the average kinetic energy is

$$\begin{aligned}
&\frac{m}{2}\left\langle\left(\frac{d\delta y_i}{dt}\right)^2\right\rangle\Bigg|_{t=\nu T+0} \\
&= \frac{m}{2}\left\langle\left\{\left.\frac{d\delta y_i}{dt}\right|_{t=\nu T-0} - \Omega_{K,\nu}\delta y_i\left(t=\nu T-0\right)\right\}^2\right\rangle \\
&= \frac{m}{2}\left\langle\left(\frac{d\delta y_i}{dt}\right)^2\right\rangle\Bigg|_{t=\nu T-0} + \frac{m}{2}\Omega_{K,\nu}^2\left\langle\left(\delta y_i\right)^2\right\rangle\Big|_{t=\nu T-0} \\
&= \frac{m}{2}\left\langle\left(\frac{d\delta y_i}{dt}\right)^2\right\rangle\Bigg|_{t=\nu T-0} + \frac{m}{2}\left(\Omega_{K,\nu}D_y/2\sqrt{3}\right)^2
\end{aligned} \quad (63)$$

where it was assumed that globally, the cloud is stationary. If in stead, (61) was used the result would have been

$$\begin{aligned}
&\left\langle\left(\frac{dy_i}{dt}\right)^2\right\rangle\Bigg|_{t=\nu T+0} \\
&= \left\langle\left\{\left.\frac{dy_i}{dt}\right|_{t=\nu T-0} + \frac{eN_{e,\nu}}{mV}\sum_{n_y=1}^{\infty}\phi_{n_y}^{(b)}\left[\frac{\pi n_y}{D_y}\cos\left(\pi n_y\frac{y_i}{D_y}\right)\right]\right\}^2\right\rangle
\end{aligned} \quad (64)$$

or explicitly, assuming that the velocity and the location of the electrons in the cloud at *impact* are not correlated then

$$\left\langle\left(\frac{dy_i}{dt}\right)^2\right\rangle\Bigg|_{t=\nu T-0}^{t=\nu T+0} = \frac{1}{2}\left(\frac{eN_{e,\nu}}{mV}\right)^2\sum_{n_y=1}^{\infty}\left[\phi_{n_y}^{(b)}\frac{\pi n_y}{D_y}\right]^2 \quad (65)$$

Thus the change in the kinetic energy is

$$\Delta E_{kick,\nu}\left[eV\right] = \frac{e}{4\pi\varepsilon_0}\frac{r_e}{D_y^2}N_{e,\nu}^2 f_K\left(\bar{b}\right)$$

$$f_K\left(\bar{b}\right) = \frac{64/\pi^2}{\left(1-\bar{b}\right)^2}\sum_{n_y=1}^{\infty}\left[\begin{aligned}&\sum_{n_x=1}^{\infty}\frac{\sin\left(\frac{\pi}{2}n_y\right)\sin\left(\frac{\pi}{2}n_x\right)}{\frac{n_x}{n_y}\left(n_x^2\frac{D_y}{D_x}+n_y^2\frac{D_x}{D_y}\right)}\\&\times\left[\cos\left(\pi n_x\bar{b}\right)-\cos\left(\pi n_x\right)\right]\end{aligned}\right]^2 \quad (66)$$

and the "kick-frequency"

$$\Omega_{K,\nu}^2 = \left(\frac{e^2N_{e,\nu}}{m\varepsilon_0 D_y^3}\frac{D_y}{c}\right)^2\frac{96/\pi^4}{\left(1-\bar{b}\right)^2}$$

$$\times\sum_{n_y=1}^{\infty}\left[\sum_{n_x=1}^{\infty}\frac{\sin\left(\frac{\pi}{2}n_x\right)\sin\left(\frac{\pi}{2}n_y\right)}{\frac{n_x}{n_y}\left(n_x^2\frac{D_y}{D_x}+n_y^2\frac{D_x}{D_y}\right)}\Lambda_{n_x}\right]^2. \quad (67)$$

APPENDIX C

In this appendix we determine the *vertical* field generated by the cloud at the location of the positron bunch. The electrostatic potential is

$$\Phi\left(x,y\right) = \sum_{n,m=1}^{\infty}\phi_{n,m}\sin\left(\pi n\frac{x}{D_x}\right)\sin\left(\pi m\frac{y}{D_y}\right) \quad (68)$$

therefore, assuming a uniform density in the cloud

$$\phi_{n_x,n_y} = -\frac{en_{ec}D_xD_y\left(2/\pi\right)^2}{\varepsilon_0\left(1-\bar{b}\right)\chi_{n_x,n_y}}\frac{2\Lambda_{n_x}}{n_xn_y}\sin^2\left(\frac{\pi}{2}n_y\right) \quad (69)$$

thus the vertical field on the bunch is after substituting the explicit expression for ϕ

$$\begin{aligned}
E_y\left(y\right) = &-\frac{en_{ec}}{4\pi\varepsilon_0}\frac{D_x}{D_y}\delta y\frac{32}{\pi}\frac{1}{1-\bar{b}} \\
&\times\sum_{n_x,n_y=1}^{\infty}\frac{\sin\left(\frac{\pi}{2}n_x\right)\sin^3\left(\frac{\pi}{2}n_y\right)}{\frac{n_x}{n_y}\left(n_x^2\frac{D_y}{D_x}+n_x^2\frac{D_y}{D_x}\right)}\Lambda_{n_x}
\end{aligned} \quad (70)$$

and consequently we may write

$$\begin{aligned}
E_y &= -\frac{en_{ec}}{4\pi\varepsilon_0}\frac{D_x}{D_y}\delta y\, f_E\left(\bar{b}\right) \\
f_E\left(\bar{b}\right) &= \frac{32}{\pi}\frac{1}{1-\bar{b}}\sum_{n_x,n_y=1}^{\infty}\frac{\sin\left(\frac{\pi}{2}n_x\right)\sin^3\left(\frac{\pi}{2}n_y\right)}{\frac{n_x}{n_y}\left(n_x^2\frac{D_y}{D_x}+n_x^2\frac{D_y}{D_x}\right)}\Lambda_{n_x}
\end{aligned} \quad (71)$$

For completeness, it is of interest to examine the also the horizontal force. Following a similar approach as above but expanding around $x = D_x/2+\delta x$ we obtain

$$\begin{aligned}
E_x = &-\sum_{n_x,n_y=1}^{\infty}\phi_{n_x,n_y}\sin\left(\frac{\pi}{2}n_y\right)\left(\frac{\pi n_x}{D_x}\right) \\
&\times\left[\cos\left(\frac{\pi}{2}n_x\right)-\delta x\frac{\pi n_x}{D_x}\sin\left(\frac{\pi}{2}n_x\right)\right].
\end{aligned} \quad (72)$$

Ignoring the term which is independent of δx (since it can be compensated by the lattice) we obtain the two "spring-coefficients" ($K_x \equiv E_x/\delta x,\ K_y \equiv E_y/\delta y$)

$$\begin{aligned}
K_x &= \sum_{n_x,n_y=1}^{\infty}\phi_{n_x,n_y}\sin\left(\frac{\pi}{2}n_x\right)\sin\left(\frac{\pi}{2}n_y\right)\left(\frac{\pi n_x}{D_x}\right)^2 \\
K_y &= \sum_{n_x,n_y=1}^{\infty}\phi_{n_x,n_y}\sin\left(\frac{\pi}{2}n_x\right)\sin\left(\frac{\pi}{2}n_y\right)\left(\frac{\pi n_y}{D_y}\right)^2
\end{aligned} \quad (73)$$

thus the ratio between these two coefficients is

$$\frac{K_x}{K_y} = \left(\frac{D_y}{D_x}\right)^2\frac{\sum_{n_x,n_y=1}^{\infty}\phi_{n_x,n_y}\sin\left(\frac{\pi}{2}n_x\right)\sin\left(\frac{\pi}{2}n_y\right)n_x^2}{\sum_{n_x,n_y=1}^{\infty}\phi_{n_x,n_y}\sin\left(\frac{\pi}{2}n_x\right)\sin\left(\frac{\pi}{2}n_y\right)n_y^2}. \quad (74)$$

Figure 14 llustrates the ratio of the two spring-coefficients. When the cloud fills the entire volume of the

beam-chamber $\left(\bar{b} \simeq 0\right)$ the ratio may be significantly smaller than unity implying the horizontal tune-shift may be significantly smaller than the vertical tune-shift. On the other hand, when the cloud does not reach the center of the beam-chamber $\left(\bar{b} \geq 0.5\right)$, the ratio of the two quantities are determined by the Laplace equation since the bunch moves in *vacuum* (contrary to the previous case where the bunch was moving in the cloud) implying that the ratio is -1. Consequently, the horizontal tune shift may be *negative* but equal in magnitude to the vertical tune-shift. One implication of this observation, is that if the horizontal tune-shift is positive (for positrons), then in the framework of this model, the information may be used to establish the electron cloud geometry (b).

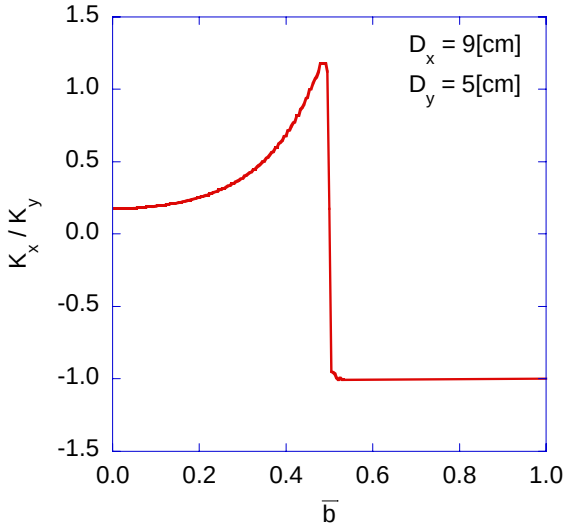

Figure 14.: The ratio of the two "spring-coefficients" as a function of the geometrical parameter. If $\bar{b} \equiv 2b/D_x \sim 0$ the cloud fills the entire bunch-chamber whereas if $\bar{b} \geq 0.5$ the bunch propagates in free-space, the magnitude of the horizontal coefficient is identical to the vertical but it is opposite in sign.

APPENDIX D

In this appendix we bring a brief but quantitative analysis of photo-emission as well as some qualitative comments on secondary emission.

Synchrotron Radiation. Let us evaluate first the number of photo-electrons generated in an energy range $E \to E + dE$ when the particles are forced to follow a circular trajectory of radius ρ. The energy in a corresponding angular frequency range is [13]

$$\frac{dW}{d\omega} \simeq 2\sqrt{3} N_e \frac{e^2}{4\pi\varepsilon_0} \frac{\gamma}{c} \frac{\omega}{\omega_{\rm cr}} \int_{2\omega/\omega_{\rm cr}}^{\infty} dx\, K_{5/3}(x) \qquad (75)$$

wherein $\omega_{\rm cr} = 3\gamma^3 c/\rho$ is the critical angular frequency and N_e represents the number of electrons in the bunch. With this expression in mind we may calculate the *total energy* emitted during one turn

$$\mathcal{E}_{\rm ph} \simeq 2\sqrt{3} N_e \frac{e^2}{4\pi\varepsilon_0} \frac{\gamma}{c} \omega_{\rm cr} \int_0^{\infty} dy\, y \int_{2y}^{\infty} dx\, K_{5/3}(x) \qquad (76)$$

The integral can be evaluated analytically $I_1 = \int_0^{\infty} dy\, y \int_{2y}^{\infty} dx\, K_{5/3}(x) = 2\pi/9\sqrt{3}$ implying that the total energy associated with the generated photons is $\mathcal{E}_{\rm ph} \simeq (4\pi/3) N_e \left(e^2/4\pi\varepsilon_0\right)\left(\gamma^4/\rho\right)$ therefore the average power generated in the process is

$$P = \frac{\mathcal{E}_{\rm ph}}{C} c \simeq \frac{2}{3} N_e \frac{e^2 c}{4\pi\varepsilon_0} \frac{\gamma^4}{\rho^2} \qquad (77)$$

$C = 2\pi\rho$ denoting the circumference of the ring. In a similar way, the *total number of photons* emitted is

$$N_{\rm ph} \simeq 2\sqrt{3} N_e \frac{e^2}{4\pi\varepsilon_0} \frac{\gamma}{c\hbar} \int_0^{\infty} d\omega \frac{1}{\omega_{\rm cr}} \int_{2\omega/\omega_{\rm cr}}^{\infty} dx\, K_{5/3}(x) \qquad (78)$$

Since the integral $I_2 \equiv \int_0^{\infty} dy \int_{2y}^{\infty} dx\, K_{5/3}(x) = 5\pi/6$ we get

$$\frac{N_{\rm ph}}{N_e} \simeq 130 \times E_k[GeV] \qquad (79)$$

Roughly, for a 2GeV beam each electron generates about 260 photons and 650 photons at 5GeV.

Spectrum of the Synchrotron Radiation. The number of photons in the energy range $E \to E + dE$ is given by

$$\tilde{N}_{\rm ph}(E) \equiv \frac{dN_{\rm ph}}{dE} \simeq 6.62 \times 10^{-2} \gamma N_e \left[\frac{6}{5\pi} \frac{1}{E_{\rm cr}} \int_{2E/E_{\rm cr}}^{\infty} dx\, K_{5/3}(x) \right] \qquad (80)$$

satisfying $\int_0^{\infty} dE \tilde{N}_{\rm ph}(E) \simeq 6.62 \times 10^{-2} \gamma N_e$ thus

$$f_{\rm ph}(E) = \frac{6}{5\pi} \frac{1}{E_{\rm cr}} \int_{2E/E_{\rm cr}}^{\infty} dx\, K_{5/3}(x) \qquad (81)$$

may be conceived to represent the "probability-density" of emitting a photon in the energy range $E \to E + dE$. The spectrum below 4eV is irrelevant since this is (roughly) the work function of *Aluminium* [14] implying that photons of lower energy will not extract photons from the material. Excluding the spectrum of photons below 4eV, the average energy drops to 67.84[eV] and 961[eV] (from 68.47[eV] and 1070[eV]) for 2 and 5GeV electrons respectively. To summarize the number of generated photons above a given threshold $E > E_{\rm th}$

$$\frac{N_{\rm ph}}{N_e} \simeq 2\sqrt{3} \frac{e^2}{4\pi\varepsilon_0} \frac{\gamma}{c\hbar} \int_{E_{\rm th}/E_{\rm cr}}^{\infty} dy \int_{2y}^{\infty} dx\, K_{5/3}(x) \simeq 49.5 \times E_k[GeV] \int_{E_{\rm th}/E_{\rm cr}}^{\infty} dy \int_{2y}^{\infty} dx\, K_{5/3}(x) \qquad (82)$$

Since the values presented in Table I were calculated for a $\rho = 80[m]$ bend this implies that *per meter* the number of photons generated is about half the number of electrons/positrons in the bunch for a 2GeV beam and roughly 1.3 photons for each electron in the 5GeV regime. Moreover, at 2GeV only 68% of the photons may generate photo-electrons but only 5% of the photons have enough energy to generate electrons that may trigger a secondary-electrons (300eV); these photons carry 4% of the total power. In the case of a 5GeV bunch, 87% of the photons may generate photo-electrons and almost 50% may generate photo-electrons with energy larger than 300eV. These carry 97% of the total photon power.

$E_{\text{th}}[eV]$	$E_k = 2[GeV]$	$E_k = 5[GeV]$
0	259.4	648.5
4	177 (68%)	565 (87%)
300	13.8(5%)	314 (48%)

Table I: The number of photons per electron for two thresholds. One corresponding to the work function of the Aluminium and the other to the peak of secondary emission in order to asses how many of the photo-electrons may become relevant to multi-pactoring.

Photo-Electrons. Denoting by $\delta_{\text{pe}}\left(E\middle|E'\right)$ the yield of generating a photo-electron of energy E by a photon of energy E' we conclude that the spectrum *photo-electrons* is

$$\tilde{N}_{\text{pe}}\left(E\right) \simeq \int_{E_{\text{w}}}^{\infty} dE'\,\delta_{\text{pe}}\left(E\middle|E'\right)\tilde{N}_{\text{ph}}\left(E'\right) \tag{83}$$

This yield depends on the properties of the material and it is independent of the properties of the bunch or the cloud. It tacitly includes information regarding *incidence angle* of the photons as well as the *reflection* process. As already indicated, only photons with energy above the threshold $\left(E_{\text{w}}\right)$ set by the *work-function* of the emitting material are being considered. At this point we may evaluate the density of photo-electrons by first defining the *average yield* $\left(\bar{\delta}_{\text{pe}}\right)$ as

$$\bar{\delta}_{\text{pe}} \equiv \int_0^{\infty} dE \int_{E_{\text{w}}}^{\infty} dE'\delta_{\text{pe}}\left(E\middle|E'\right) f_{\text{ph}}(E') \tag{84}$$

implying that the total number of photo-electrons is

$$\begin{aligned}\bar{N}_{\text{pe}} &= \int_0^{\infty} dE\tilde{N}_{\text{pe}}\left(E\right) \simeq \int_0^{\infty} dE' \int_{E_{\text{w}}}^{\infty} dE'\delta_{\text{pe}}\left(E\middle|E'\right)\tilde{N}_{\text{ph}}\left(E'\right) \\ &= 6.62\times 10^{-2}\gamma N_e \int_0^{\infty} dE' \int_{E_{\text{w}}}^{\infty} dE'\delta_{\text{pe}}\left(E\middle|E'\right) f_{\text{ph}}\left(E'\right) \\ \frac{\bar{N}_{\text{pe}}}{N_e} &= 130\times E_k[GeV]\,\bar{\delta}_{\text{pe}}\end{aligned} \tag{85}$$

Since the volume of the ring is $D_x D_y C$, the average density is $\bar{n}_{\text{pe}} \simeq 6.62\times 10^{-2}\gamma\bar{\delta}_{\text{pe}}\left(N_e / D_x D_y C\right)$. The number of photo-electrons above an arbitrary threshold energy E_{th} is

$$\frac{\bar{N}_{\text{pe}}}{N_e} = 130\times E_k[GeV]\int_{E_{\text{th}}}^{\infty} dE \int_{E_{\text{w}}}^{\infty} dE'\delta_{\text{pe}}\left(E\middle|E'\right) f_{\text{ph}}\left(E'\right) \tag{86}$$

At this stage we need to develop a realistic estimate of the photo-electrons energy spectrum and for this purpose, four assumptions are made:

a. According to Groebner [9] the yield of photo electrons as a function of the impinging photon energy (Aluminium) was found experimentally

$$\delta_{\text{pe}}\left(E\middle|E'\right) \propto Y(E') = \left(\frac{E_0}{E'}\right)^{\nu} \tag{87}$$

the typical parameters being $E_0 = 2.316[eV]$, $\nu = 0.825$.

b. The energy of the photo-electron should not exceed the energy of the incident photon and we further assume that the electrons' energy is *uniformly* distributed between $0 < E < E'$ hence

$$\delta_{\text{pe}}\left(E\middle|E'\right) \propto \frac{1}{E'}\left[h(E) - h(E - E')\right] \tag{88}$$

c. There is zero contribution from photons of energy lower than the work function of the metal

$$\delta_{\text{pe}}\left(E\middle|E'\right) \propto h\left(E' - E_{\text{w}}\right) \tag{89}$$

d. Not all the photons are absorbed by the surface. Consider an incident field of amplitude 1 and incident energy E' the reflection coefficient is denoted by $\rho(E')$ we conclude that the *net power* impinging upon the surface is proportional to $1 - \left|\rho_{\text{eff}}\left(E'\right)\right|^2$ therefore,

$$\delta_{\text{pe}}\left(E\middle|E'\right) \propto \left[1 - \left|\rho_{\text{eff}}\left(E'\right)\right|^2\right] \tag{90}$$

tacitly assuming that ρ is the average over the relevant range of angles of incidence. Note that the photons generated by the beam may be reflected but being confined by the vacuum pipe they eventually impinge again on the metallic wall. The reflection coefficient accounts for the *overall reflection events*. With these assumptions in mind, the overall yield reads

$$\begin{aligned}\delta_{\text{pe}}\left(E\middle|E'\right) \simeq Y\left(E'\right)\frac{1}{E'}&\left[h(E) - h(E - E')\right] \\ &\times h\left(E' - E_{\text{w}}\right)\left[1 - \left|\rho_{\text{eff}}\left(E'\right)\right|^2\right]\end{aligned} \tag{91}$$

implying that

$$\frac{\bar{N}_{\rm pe}}{N_e} = 49.54\times E_k[GeV]\left(\frac{E_0}{E_{\rm cr}}\right)^{\nu}\int\limits_{E_{\rm th}/E_{\rm cr}}^{\infty} dx \times \int\limits_{\max\left(x,\frac{E_{\rm w}}{E_{\rm cr}}\right)}^{\infty} dy\, y^{-\nu-1}\left[1-\left|\rho_{\rm eff}\left(yE_{\rm cr}\right)\right|^2\right]\int\limits_{2y}^{\infty} du\, K_{5/3}(u) \tag{92}$$

According to the estimate of the multi-reflection process in Appendix E the effective reflection coefficient is

$$\left|\rho_{\rm eff}(E)\right|^2 \simeq \left(\frac{D_x}{2^5\rho}\right)^{1/4}\theta_{\rm cr}(E)\exp\left[-\frac{\pi\sqrt{2}}{\theta_{\rm cr}^2(E)}\sqrt{\frac{D_x}{\rho}}\right] \tag{93}$$

wherein $\theta_{\rm cr} = 18.85\sqrt{\rho_M[{\rm gr/cm^3}]}/E[eV]$ and ρ_M is the material weight density [15]. For Aluminium and $D_x = 9[{\rm cm}], \rho = 80[{\rm m}]$ the effective reflection coefficient is

$$\left|\rho_{\rm eff}(E)\right|^2 \simeq \frac{1.881}{E}\exp\left(-1.2486\times10^{-4}E^2\right) \tag{94}$$

Examining the argument of the exponent, we clearly conclude that photons with energies higher than 100eV are absorbed at the first impact.

The table below summarizes the number of photo-electrons generated with and without the reflection process accounted for 2GeV and for the following set of parameters: $E_{\rm th} = 4[{\rm eV}]$, $E_0 = 2.316[{\rm eV}]$, $D_x = 9[{\rm cm}]$, $\rho = 80[m]$ and $\rho_M = 2.375[{\rm gr/cm^3}]$

	$E_{\rm th}[eV]$	$E_k = 2[GeV]$	
		$\rho_{\rm eff}(E) = 0$	$\rho_{\rm eff}(E) \neq 0$
$N_{\rm pe}/N_e$	0	25.8	20.9
	300	0.05(0.2%)	0.05(0.2%)
$\bar{\delta}_{\rm pe}$	0	1.0×10^{-1}	0.8×10^{-1}
	300	1.8×10^{-4}	1.8×10^{-4}

Table II: The number of photo-electrons

The results in Table II indicate that for 2GeV electrons, the number of photo-electrons relevant to sustainable secondary emission is small (less than 0.05 out of 21-26). The maximum yield is of the order of 0.1 .

APPENDIX E

For an estimate of the reflection coefficient (single reflection) we shall assume that below a critical angle $\theta \le \theta_{\rm cr} = 18.85\sqrt{\rho_M[{\rm gr/cm^3}]}/E[eV]$ wherein $\rho_M\left[{\rm gr/cm^3}\right]$ is the material weight density, the reflection coefficient is virtually unity and zero otherwise or explicitly $\left|\rho(E,\theta)\right| \simeq \exp\left[-\theta^2/2\theta_{\rm cr}^2(E)\right]$. For a single reflection we may conclude [16] that

$$\left|\rho(E)\right|^2 \simeq \int_0^{\infty} d\theta\exp\left[-\theta^2/\theta_{\rm cr}^2(E)\right] \simeq \frac{1}{2}\sqrt{\pi}\theta_{\rm cr}(E) \tag{95}$$

implying

$$\tilde{N}_{\rm pe}(E) \simeq 6.62\times10^{-2}\frac{\gamma N_e}{E_{\rm cr}}\left(\frac{E_0}{E_{\rm cr}}\right)^{\nu}\int\limits_{\max(E,E_{\rm th})}^{\infty} dE' \times\left(\frac{E_{\rm cr}}{E'}\right)^{\nu+1} f_{\rm ph}(E')\left[1-\frac{\pi}{4}\left(18.85\frac{\sqrt{\rho_M}}{E'}\right)^2\right] \tag{96}$$

It is necessary to account for the spectrum which is not absorbed in the wall and continues to bounce between the walls i.e., in case of multiple reflections. For this purpose let us assume a beam-chamber of rectangular cross section $\left(D_x\times D_y\right)$ and radius of curvature $\rho \gg D_x, D_y$; moreover we focus our attention to the horizontal plane (*x*). Denoting by θ_n the angle of exit from the n'th reflection -- see Figure 15

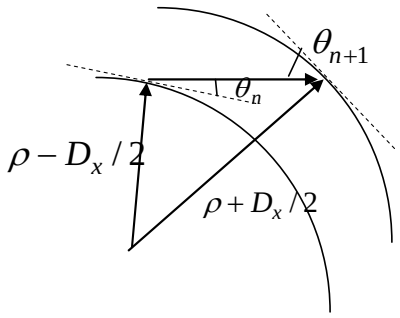

Figure 15.: Scattering of synchrotron radiation at small angles.

and by θ_{n+1} the angle of incidence of the next reflection. Based on this simple model we may readily conclude that $\theta_{n+1}^2 = \theta_n^2 + D_x/\rho$. In case of two reflections we have

$$\left|\rho(E)\right|^2 \simeq \int_0^{\infty} d\theta\exp\left(-\frac{\theta^2}{\theta_{\rm cr}^2}\right)\exp\left[-\frac{\theta^2+D_x/\rho}{\theta_{\rm cr}^2}\right] \simeq \frac{1}{2}\sqrt{\pi}\frac{\theta_{\rm cr}(E)}{\sqrt{2}}\exp\left[-\frac{D_x/\rho}{\theta_{\rm cr}^2(E)}\right] \tag{97}$$

In a similar way, in case of $2N$ reflections (N from each boundary) we get

$$\left|\rho_{\rm eff}(E)\right|^2 \simeq \int_0^{\infty} d\theta\left\{\exp\left[-\frac{\theta^2}{\theta_{\rm cr}^2(E)}\right]\exp\left[-\frac{\theta^2+D_x/\rho}{\theta_{\rm cr}^2(E)}\right]\right\}^{N+1} \simeq \frac{1}{2}\sqrt{\pi}\frac{\theta_{\rm cr}(E)}{\sqrt{2(N+1)}}\exp\left[-\frac{2(N+1)a_x/\rho}{\theta_{\rm cr}^2(E)}\right] \tag{98}$$

The number of reflections may be approximated based on Figure 15 by

$$N+1 \simeq \frac{2\pi\rho}{2\sqrt{\left(\rho+\frac{D_x}{2}\right)^2-\left(\rho-\frac{D_x}{2}\right)^2}} \simeq \sqrt{\frac{\pi^2\rho}{2D_x}} \qquad (99)$$

hence

$$\left|\rho_{\text{eff}}(E)\right|^2 \simeq \left(\frac{D_x}{2^6\rho}\right)^{1/4} \theta_{\text{cr}}(E)\exp\left[-\frac{\pi}{\theta_{\text{cr}}^2(E)}\sqrt{\frac{D_x}{\rho}}\right] \qquad (100)$$

REFERENCES

1. M. Izawa, Y. Sato and T. Toyomasu; “The vertical instability in a positron bunched beam”, Phys. Rev. Lett., 74, 5044-7 (1995).
2. K. Ohmi; “Beam-Photoelectron Interaction in Positron Storage Rings”, Phys. Rev. Lett., 75, 1526-9 (1995).
3. K. Ohmi and F. Zimmermann; “Head-Tail Instability Caused by Electron Clouds in Positron Storage Rings”, Phys. Rev. Lett., 85, 3821-4 (2000).
4. H. Fukuma; “Electron Cloud Effects at KEKB”, Proceedings of ECLOUD’02 Workshop, CERN, 15-18 April 2002. http://wwwslap.cern.ch/collective/ecloud02/proceedings/index.html http://conf-ecloud02.web.cern.ch/conf-ecloud02/papers/allpdf/fukuma_rev.pdf
5. J. W. Flanagan, K. Ohmi, H. Fukuma, S. Hiramatsu and T. Tobiyama; “Observation of Vertical Betatron Sideband due to Electron Clouds in the KEKB Low Energy Ring”, Phys. Rev. Lett. 94, 054801 (2005).
6. I. Hofmann; Beam Dynamics Newsletter, No. 41, Editor in Chief W. Chou, International Committee for Future Accelerators (ICFA), December 2006; in particular see Table 1 (p. 67) in the note by F. Zimmermann. http://www-bd.fnal.gov/icfabd/Newsletter41.pdf
7. A.Z. Ghalam, T. Katsouleas, V.K. Decyk, C.K. Huang, W.B. Mori, G. Rumolo, E. Benedetto and F. Zimmermann; “Three-dimensional continuous modeling of beam-electron cloud interaction: comparison with analytic models and predictions for the present and future circular machines”, Physics of Plasmas, 13, 056710 (2006).
8. K. Ohmi, S. Heifets and F. Zimmermann; “Study of Coherent Tune-Shift Caused by Electron Cloud in Positron Storage Rings”, Proceedings of the Second Asian Particle accelerator Conference, Beijing, China (2001) p.445.
9. O. Grobner et al., J. Vac. Sci. Technolo. A 7 p. 223-9 (1989) "Neutral gas desorption and photoelectric emission from aluminum alloy vacuum chambers exposed to synchrotron radiation" in particular see p.224 (Figure 2)
10. M. Furman and M. Pivi (PRSTAB, 5, 124404).
11. J. R. M. Vaughan, "A new Formula for Secondary Emission Yield", IEEE Transactions on Electron Devices Vol 36 (9) p.1963 (1989). This being a variant of: R.G. Lye and A.J. Dekker, "Theory of Secondary Emission", Physical Review Vol. 107, pp.977-981 (1957).
12. According to CRC Handbook of Chemistry and Physics, 48-Edition (p. E-152) for Al_2O_3 this value may vary from 2 to 9 !!
13. J.D. Jackson; "Classical Electrodynamics", John Wiley and Sons, New York, Second Edition - 1975, p.677
14. $W_{100} = 4.20[\text{eV}], W_{110} = 4.06[\text{eV}], W_{111} = 4.26[\text{eV}]$ according to "Handbook of Chemistry and Physics", Edited by David R. Lide, 80th Edition 1999-2000, CRC Press, Bocca Raton.
15. $\rho_M = 2.375[\text{gr/cm}^3]$ "Handbook of Chemistry and Physics", Edited by David R. Lide, 80th Edition 1999-2000, CRC Press, Bocca Raton.
16. Handbook of X-rays, edited by E.F. Kaelble, McGraw-Hill, New York, 1967, p. 48-2 $\theta_{\text{cr}} = 1.6\times10^5\lambda[\text{cm}]\sqrt{\rho_M\left[\text{gr/cm}^3\right]}$.